ANALYTICAL AND NUMERICAL SENSITIVITY ANALYSIS OF CONSTANT TEMPERATURE HOT-WIRE ANEMOMETRE

A Thesis Submitted to
the Graduate School of Engineering and Science of
İzmir Institute of Technology
in Partial Fulfillment of the Requirements for the Degree of

MASTER OF SCIENCE

in Mechanical Engineering

by
Yusuf Can UZ

July 2014
İZMİR

We approve the thesis of **Yusuf Can UZ**.

Examining Committee Members:

_____

Assist. Prof. Dr. Ünver ÖZKOL
Department of Mechanical Engineering
İzmir Institute of Technology

_____

Assoc. Prof. Dr. Moghtada MOBEDİ
Department of Mechanical Engineering
İzmir Institute of Technology

_____

Assoc. Prof. Dr. Tahsin BAŞARAN
Department of Architecture
İzmir Institute of Technology

9 July 2014

_____

Assist. Prof. Dr. Ünver ÖZKOL
Supervisor, Department of Mechanical Engineering
İzmir Institute of Technology

_____

Prof. Dr. Metin TANOĞLU
Head of the Department of
Mechanical Engineering

_____

Prof. Dr. R. Tuğrul SENGER
Dean of the Graduate School of
Engineering and Sciences

ACKNOWLEDGMENTS

This thesis is dedicated to my family Sait Ali and Naide UZ, who have always believed me. I would like to thank to my family for their constant encouragement and support.

I would like to thank to my advisor, Dr. Ünver ÖZKOL, for his constant support throughout dissertation. His continuous guidance is greatly appreciated. I am also grateful to the other committee members for the guidance.

I would like to thank to Assist. Prof. Dr. Levent AYDIN, for his endless effort to teach all his computer programming knowledge to me.

I would like to appreciate deeply my colleague Çağlar COŞKUN, Egemen AĞAKAY, Mutlu Devran YAMAN and Serkan KANGAL for their support during the investigations and report of the thesis.

Finally, I would like to express my special thanks to my friends Emrah, Erdem, Mehmet, Zehra, Çisem, Gizem, Hamza, Levent, Sırma, Aysel and others for their encouragement, support and patience during this graduate work.

ABSTRACT

ANALYTICAL AND NUMERICAL SENSITIVITY ANALYSIS OF CONSTANT TEMPERATURE HOT-WIRE ANEMOMETRE

Hot-wire anemometry (HWA) has been used for many years as a research tool in fluid mechanics. HWA consists of a wire sensor, a very fine element exposed to the fluid flow and of an electronic system, which performs the transformation of the sensor output into a useful electric signal. HWA is based on convective heat transfer from a heated wire which is placed into a fluid flow. The heat is generated inside the very fine wire owing to wire resistance when electrical current passes through it. Then, the wire will be subjected to heat losses by convection, conduction and radiation depending on the flow condition. To examine the theory of operation for the heated wire and plot the temperature distribution along it, energy balance for HWA is investigated by taking differential element of dx length of the filament. In order to understand static and dynamic characteristics of hot-wire, all kinds of heat transfer such as convection, conduction and radiation are taken into consideration. In present thesis, the static study starts to investigate influence of the sensor parameters on general behavior of the constant temperature hot-wire anemometer analytically and numerically at varying conditions. Most important part of this study is that the time dependent differential equation for the heated wire is solved to determine sensitivity of hot-wire by a perturbation method in the event of a harmonically changing heat transfer coefficient. Moreover, the influence of thin supporting wires, or copper plated wire ends, is evaluated to see the effects of them on sensitivity and heat dissipation to the prongs. Another important parameter for wire sensor is the aspect ratio (L/d). Aspect ratio affects the time constant, sensitivity and temperature distribution of heated wire; hence it needs to be examined. Also, effect of the various velocities on the temperature distribution and sensitivity along the hot-wire has been studied.

ÖZET

SABİT SICAKLIK SICAK TEL ANEMOMETRE HASSASİYETİNİN ANALİTİK VE NÜMERİK ANALİZİ

Sıcak tel anemometresi, uzun yıllardır akışkanlar mekaniğinde bir araştırma cihazı olarak kullanılmaktadır. Sıcak tel anemometresi bir akışkan akımına maruz bırakılan küçük bir teli olan sensör ve sensor çıkışını ölçülebilir bir elektrik sinyaline dönüştüren elektronik bir donanıma sahiptir. Sıcak tel anemometresi, akışkan ortamına yerleştirilmiş bir sıcak tel elemanından konvektif (taşınım) ısı transferini esas alır. Isı, elektrik akımı geçtiğinde tel direnci nedeniyle bu çok ince telin içinde üretilir. Isının telden çevreye iletilmesi akış koşullarına bağlı olarak iletim, konveksiyon ve radyasyon yolu ile olur. Sıcak tel anemometresinin çalışma prensibini ve tel boyunca sıcaklık dağılımını incelemek için dx uzunluğundaki diferansiyel bir elemanın ısıl dengesi incelenmiştir. Sıcak telin statik ve dinamik özelliklerini anlamak için konveksiyon, iletim ve radyasyon olmak üzere tüm ısı transferleri dikkate alınmıştır. Statik çalışma, sensör parametrelerinin değişen koşullarda sıcak tel anemometresi üzerindeki etkisinin analitik ve nümerik çalışmalarını içerir. Bu çalışmanın en önemli kısmı, hassasiyet hesapları için zamana bağlı diferansiyel denklemin tedirgileme kuramı ile çözümlenmesidir. Bu method kullanılırken ısı tranferi katsayısı zamana bağlı, harmonik olarak değişmektedir. Buna ek olarak, destek iğnelerinin ince veya bakır kaplı olmasının, telin hassasiyeti ve bu iğnelere iletim ile aktarılan ısı üzerindeki etkileri incelenmiştir. Bir sıcak tel anemometresinde sensörün boyu ve çapı arasındaki ilişki önemlidir. Görüntü oranı, zaman sabitini, hassasiyeti ve sıcaklık dağılımını etkilediği için incelenmesi gerekmektedir. Ayrıca, hız değişimlerinin hassasiyet ve sıcaklık dağılımı üzerindeki etkisi çalışılmıştır.

TABLE OF CONTENTS

LIST OF FIGURES

LIST OF TABLES

LIST OF SYMBOLS

T	$T^{'} - T_a$	°C
$T^{'}$	Local temperature of the wire	°C
T_w	Wire temperature	°C
$T_{w,m}$	Constant mean temperature imposed by the anemometer circuit	°C
T_{cu}	Local difference between the temperature of the supporting wires and the ambient temperature	°C
T_a	Ambient temperature	°C
T_f	Film temperature	°C
T_m	Mean temperature	°C
f	$\pi\ D\ h$	W/m K
g	$I^2 R_0$	W/m
p	$\frac{1}{4}\pi\ D^2 \rho\ c_w$	W/m
q	$\frac{1}{4}\ \pi\ D^2\ k$	kJ/kg K
D	Diameter of the wire	µm
d	Diameter of the wire	µm
L	Length of the wire	mm
l	Length of the wire	mm
L_s	Whole length of the active and copper-plated portion of the wire	mm
c_w	The specific heat of the wire	cal/g °C
c_{cu}	The specific heat of the copper-plated ends of the wire	cal/g °C
k	Thermal conductivity	W/(m K)
k_w	Thermal conductivity of wire	W/(m K)
k_f	Thermal conductivity of the fluid	W/(m K)
k_{cu}	Thermal conductivity of copper-plated ends of wire	W/(m K)
h	Heat transfer coefficient	W/(m^2 K)
h_{cu}	Heat transfer coefficient of the copper-plated ends of the wire	W/(m^2 K)

ρ	Density	kg/m^3
ρ_{cu}	Density of the copper-plated ends of the wire	kg/m^3
I	Electrical current	mA
R_w	Electrical resistance of the wire	Ω
R_0	Electrical resistance of the wire at 0 °C	Ω
β	Temperature coefficient of the resistance at T_f	1/°C
A	Cross section area	m^2
A_w	Cross section area of the wire	m^2
ω	Circular frequency	1/s
τ	Time constant	s
τ_{cu}	Time constant of the copper-plated ends of the wire	s
γ_0	Electrical resistivity at 0 °C	Ω m
γ_a	Electrical resistivity at T_a	Ω m
φ	Ratio of the convective heat transfer to the conduction to the prongs.	
α_0	Temperature coefficient of resistivity at 0 ℃.	1/°C
Nu	Nusselt number	
Re	Reynold number	
Ma	Mach number	
Gr	Grashof number	
Pr	Prandtl number	
$\dot{Q}_e$	The electrical heat-generation rate	W
$\dot{Q}_{fc}$	The forced-convective heat-transfer rate	W
$\dot{Q}_c$	The conductive heat-transfer rate	W
$\dot{Q}_r$	The radiation heat-transfer rate	W
$\dot{Q}_s$	The heat storage rate	W
P	Electric power input to sensor	W
H	Heat transfer from sensor to environment	W
t	Time	s
ε	Small parameter	
σ	Stefan-Boltzmann constant	$Wm^{-2}K^{-4}$
ϵ	The emissivity of the sensor material	

c_p	Specific heat of fluid at constant pressure	kJ/kg °C
c_v	Specific heat at constant volume	kJ/kg °C
μ	Dynamic fluid viscosity	kg/m s
ϑ	Kinematic fluid viscosity	m^2/s
U	Free stream velocity	m/s
β_v	Volume coefficient of expansion	K^{-1}
c	Speed of sound	m/s
α_1	Angle between free-stream flow direction and normal to cylinder	◦
γ_h	C_p/C_v	
a_T	Overheat ratio or temperature loading	

CHAPTER 1

INTRODUCTION

Flow measurement has a history of about 3000 years. Since ancient times, flow measurement is a sign of human civilization. Egyptians use the Nile River flow meter to predict the harvest is good or bad. Roman drainage pipes and water measured by orifice flow. The ancient Sumerian cities of UR and Kish, near the Tigris and Euphrates rivers (around 5000 B.C.) used water flow measurement to manage the flow of water through the aqueducts in their cities. In this age a simple obstruction was placed in the water flow, and by measuring the height of the water flowing over the top of the obstruction, those engineers could determine how much water was flowing. In 1450 the Italian art architect Battista Alberti invented the first mechanical anemometer (see Figure 1.1). It consisted of a disk placed perpendicular to the wind, and the force of the wind caused it to rotate. The angle of inclination of the disk would then indicate the wind velocity. This was the first recorded instrument to measure wind speed. An English inventor, Robert Hooke reinvented this device in 1709, along with the Mayan Indians around that same period of time. As can be seen in these developments and events, flow measurements play important role for their benefits.

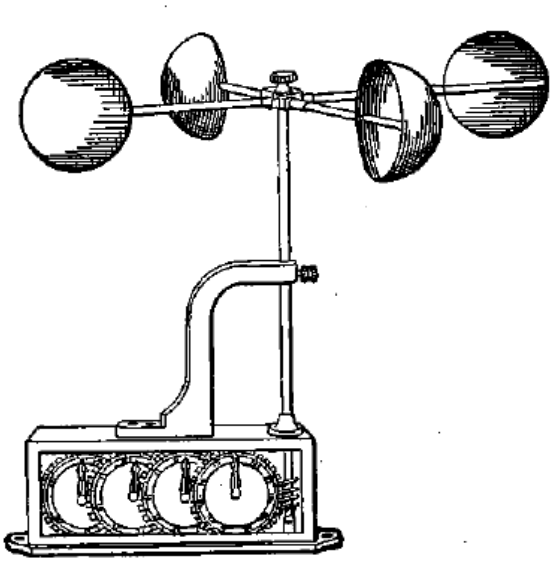

Figure 1.1.Mechanical Anemometer

From past to present, fluid flow measurements have importance in processes occurring in our environment, areas of; Agriculture, Civil engineering, Oceanography, Aerospace, Automotive, Bio-medical & bio-technology, Combustion diagnostics, Earth science & environment, Fundamental fluid dynamics, Hydraulics & hydrodynamics, Mixing processes, Process & chemical engineering, Wind engineering, Experimental physics and many other engineering areas where there is a fluid flow.

While taking these measurements, almost all industrial and human-made flows are turbulent. Almost all naturally occurring flows on earth, in oceans, in seas, and atmosphere are turbulent. So, measurement and investigation of turbulent characteristics has great importance. In making turbulent measurements, it is not a question of the best instrument but rather which instrument will perform best for the specific application.

1.1. Hot-Wire Anemometry

Hot-Wire Anemometry (HWA) has been used for many years as a research tool in turbulent air/gas studies (Bruun, 1996). It is still applied in many application areas owing to improvements of electronic technology. HWA is a kind of thermal anemometer which computes flow velocity by its relationship between local flow velocity and the heat transfer from heated element. Thermal anemometer provides an analogue output which represents the velocity in a point. Velocity information is thus available anytime. They are suitable for learning about flow details, especially in turbulent flow due to their small size and good frequency response. Furthermore, the hot wire anemometer is still the only instrument delivering at the output a truly analogue representation of the velocity up to high frequencies.

The hot wire anemometer consists of a sensor, small electrically heated wire exposed to the fluid flow and of electronic equipment which performs the transformation of the sensor output into a useful electric signal. In contrast to most measuring instruments, electronic circuitry forms an integral part of the anemometric system and has a direct effect on the probe. In Figure 1.2, electronic part and probe of the hot wire is basically given.

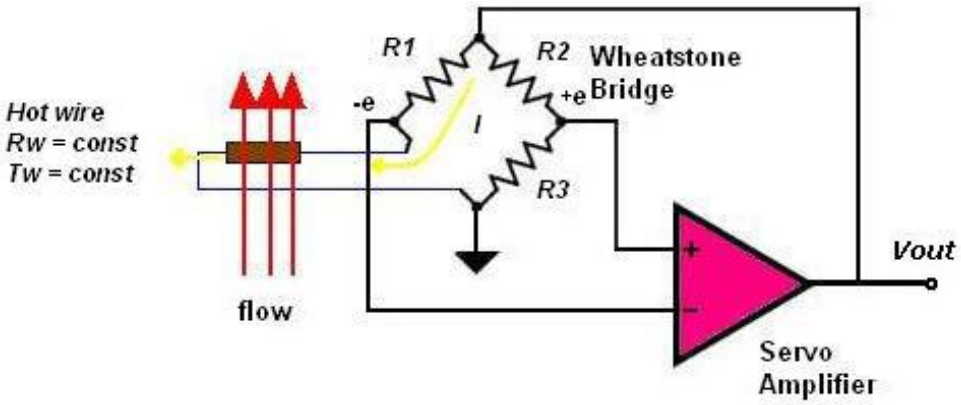

Figure 1.2. Elementary form of the hot-wire anemometer.

The basic principle of operation of the system is the heat transfer from the heated wire to the cold surrounding fluid, heat transfer which is function the velocity. Therefore, HWA is based on convective heat transfer from the heated wire. The heat is generated inside the wire owing to wire resistance when electrical current passes through it.

1.2. Strengths, Limitations and Comparisons

Properties of an ideal instrument are summarized by Goldstein (1996) and they are as follows;

1. Have high-frequency response to accurately follow transients
2. Be small in size for an essentially point measurement
3. Measure a wide velocity range
4. Measure only velocity, and work in a wide range of temperature, density, and composition
5. Measure velocity components and detect flow reversal
6. Have high accuracy
7. Have high resolution
8. Create minimal flow disturbance
9. Be low in cost
10. Be easy to use

For a long time, the hot wire anemometer has satisfied most of those criteria to measure velocity details in turbulence studies. Pitot probes, flow visualization, and other techniques have been used for studies but could not get details as well as the hot wire. Since its introduction in 1964 (Yeh & Cummins, 1964), the use of laser velocimetry has begun to spread in flow experiments with developments of lasers. Laser Doppler anemometry (LDA), is the technique of using the Doppler shift in a laser beam to measure the velocity of particles in transparent or semi-transparent fluid flows. Those and the fact that the measurement point must be in optically accessible is a drawback of laser methods compared to the HWA. Both of LDA and HWA are point measurement technique and can offer good spatial and temporal response. This makes them ideal for measurements of both time-independent flow statistics, such as moments of velocity (mean, rms, etc) and time-dependent flow statics such as spectra and correlation functions at a point.

There are several advantages of conventional HWA for measurements in low and moderate turbulence intensity flows (less than ~ 25%). In following, HWA and LDA are compared on the basis of some criteria for the ideal instrument (Goldstein, 1996).

1. *Cost*. HWA systems are cheaper than other main competitors, Laser Doppler Anemometers (LDAs).
2. *Frequency response.* Measurements up to several hundred kilohertz are easy to obtain. Theoretically, LDA can come near the response of thermal anemometry, but practically it is up to 30 kHz. At high frequencies, electronic limitations generate technical barriers for LDAs.
3. *Size.* Typical hot-wire type sensor is 5 μm in diameter and 2 mm in long. Also, subminiature sensor is 1 μm in diameter and 0.25 mm in long. In contrast, measuring volume is 50 μm by 0.25 mm for a laser velocimeter.
4. *Velocity range*. Both techniques have wide range of velocity. At very low velocities, "free convection" affects hot-wire readings badly, but there is no such a problem in Laser Doppler.

   Laser data are easier to figure out because they focus only particle velocity and no calibration is required.
5. *Measure velocity over wide temperature density and composition range.* Laser Doppler measures only velocity of particle in a known direction. HWA can measure velocity and temperature at the same time with two sensors. Both

instruments could work over wide temperature, density, and composition ranges. At low density, it is hard to get reliable results. For hot-wire anemometry, conduction losses affect measurements

6. *Component resolution.* The hot wire can include one, two or three sensor. Because of this reason, it can be used to resolve one, two or all three components of the flow. It is difficult to obtain all component of velocity with Laser Doppler, it needs separate lens system.
7. *Accuracy.* Hot wire results are repeatable, so accuracy depends on calibration conditions which are rebuilt in the flow to be measured. If carefully controlled experiments are carried out, both HWA and LDA give very accurate results (0.1%-0.2%). However, in many practical applications, accuracy is nearby 1%.
8. *Resolution.* Thanks to the low noise, the hot wire is clearly superior. Resolution of 1 part in 10 000 is easily accomplished, while with a LDA 1 part in 1000 is difficult with present technology.
9. *Flow disturbance.* In LDA systems, only light enter the flow. Owing to this, the laser is better for avoiding flow disturbance.

1.3. Probe Types

The probes may have one, two, or three sensors for use in one-, two-, or three-dimensional flow respectively. Information about magnitude and direction of velocity can be obtained with probes having two or more sensors. The sensor can either be a thin wire suspended between two prongs or a thin metal film deposited on an electrically insulating substrate. There are generally three types of hot wire as a single cylindrical sensors, X-probes and tri-axial probes. Hot-film sensors are mentioned below the hot wire types.

1.3.1. **Single Cylindrical Sensors**

Single sensor which is shown in Figure 1.3 is used for one-dimensional, uni-directional flows. They are available with different prong geometry, which allows the probe to be mounted correctly with the sensor perpendicular and prongs parallel with the flow.

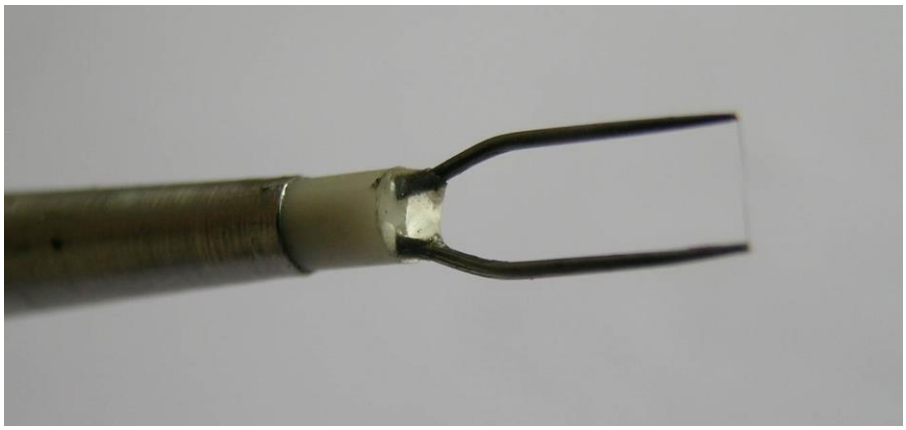

Figure 1.3. Single (Normal) wire probe.

1.3.2. **X-Probes**

Two sensors are perpendicular to each other (see Figure 1.4). It is used for two-dimensional flows and measures within $\pm 45°$. By this way, information about magnitude and direction of velocity can be easily obtained by using probes having 2 sensors.

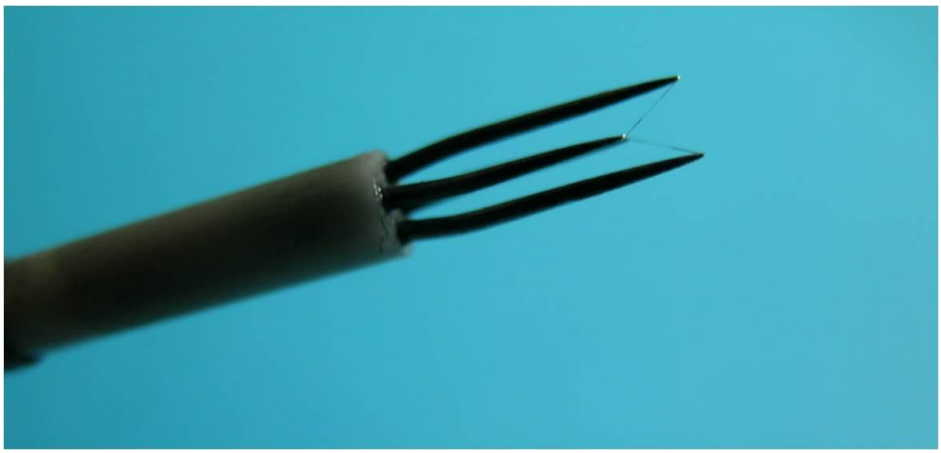

Figure 1.4. Crossed wires probe.

1.3.3. **Tri-Axial Probes**

Three sensors are in an orthogonal system (see Figure 1.5). It is used for three-dimensional flows and measures within $\pm 70°$. Again, information about magnitude and direction of velocity can be easily obtained by using probes having 3 sensors.

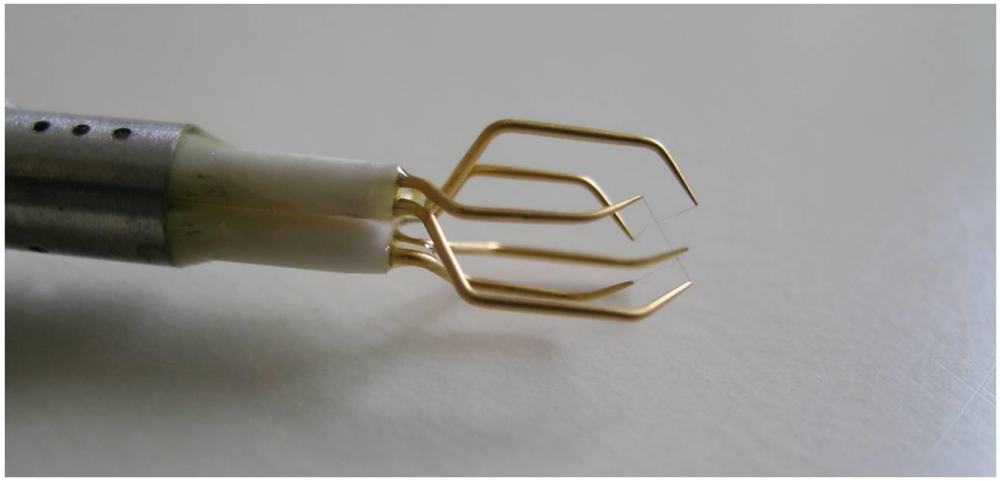

Figure 1.5. Orthogonal wires probes.

1.3.4. **Hot-Film Sensors**

The hot film sensor is essentially a conducting film laid on a ceramic or quartz substrate. The sensor can be typically, a quartz rod coated with a platinum film. The most common substrate shapes are cylinders, wedges and cones, as shown in Figure 1.6. The films are deposited by cathode sputtering to achieve a uniform thickness of the sensing element. The film sensing element is shown schematically in Figure 1.7.

The metal film thickness on a typical film sensor is less than 0.1 μm. Therefore, the mechanical strength and the effective thermal conductivity of the sensor are determined almost entirely by the substrate material. This coating protects the film material from abrasive particles. Also, it provides electrical insulation for the hot-film probes used in liquids. For the cylindrical hot-film probes, the active element is usually 25-50 μm in diameter and 1-2 mm in length.

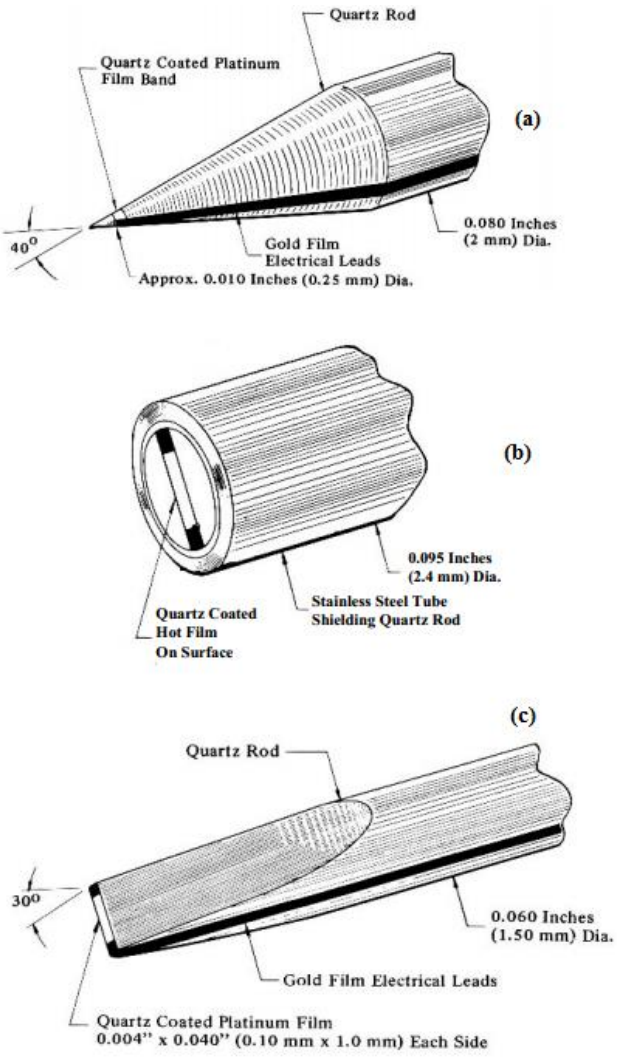

Figure 1.6. Hot-film probe types: (a) cone, (b) flush mounted, and (c) wedge. (Source: Lomas, 2011)

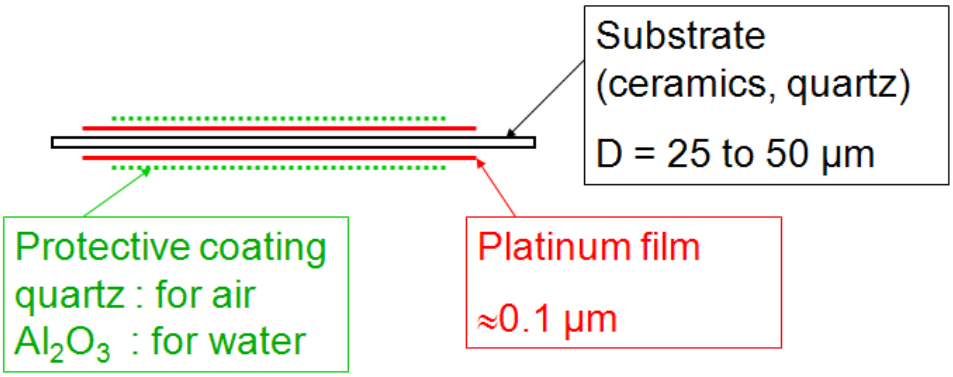

Figure 1.7. Elements of hot-film.

When detailed results of turbulence are needed, hot-wire probes are normally recommended. Better frequency response makes it more sensitive to fluctuations. Hot-film probes are usually used for liquid measurement due to their stronger construction. When hot-wire probes are compared to hot-film probes, following conclusions can be listed as:

- Hot-wire sensors provide superior performance in many applications.
- Hot-film typically has a larger diameter, and therefore a lower resolution.
- If maximum frequency response, minimum noise level and very close proximity to a surface are required, hot-wire probes will be superior.
- Hot-film is more robust than hot-wire.
- Hot-film is less sensitive to dirt and is easier to clean.
- Hot-film has a more complex material.

1.4. Hot-Wire Filaments

The most common materials employed for hot-wire filaments are tungsten, platinum and platinum-iridium (80% Pt, 20% Ir), although other materials such as iridium and nickel are used for special purposes. These material are used for hot-wire anemometry applications because of their mechanical properties but also because of their accessibility in the small sizes. Some of their properties can be seen in Table 1.1. Ideally, following properties are required:

- A high value of the temperature coefficient of resistance, to increase its sensitivity to velocity variations
- A high enough tensile strength to withstand the aerodynamics stresses at high flow velocities
- A low conductivity to bring down conduction losses to the supports.
- A low resistivity
- Availability in small diameters
- Good oxidation resistance
- High specific resistance

Table 1.1. Properties of hot-wire materials

Properties	Tungsten	Platinum	80% Platinum, 20% Iridium
Temperature coefficient of resistance α, $°C^{-1}$	0.0045	0.0039	0.0008
Resistivity, Ω.cm	5.5×10^{-6}	10×10^{-6}	31×10^{-6}
Ultimate tensile strength, Kg/mm^2	420	24.6	100
Thermal conductivity, cal/(cm.°C)	0.47	0.1664	0.042

Tungsten wire is mechanically the strongest of the common materials, and is therefore especially suited to homemade probes. Disadvantages of tungsten are that operating temperature of the wire must be limited to about 300°C to prevent oxidation, and that tungsten cannot be soft soldered (Lowell, 1950). So it must be either spot welded to the supports or else plated with copper before soft soldering to the supports.

Platinum can be soft soldered. Also, it is available in size down to 0.25 μm. But platinum is considerably more fragile than tungsten for the same size. This wire is produced by the Wollaston process which leaves a heavy coating of silver around the core wire. The silver jacket builds up the diameter of the wire to about 50 μm, which facilitates handling the material, but the silver must be etched away from the core with a nitric acid solution. Platinum can withstand operating temperature up to 800°C, and is therefore especially suitable for high temperature applications.

Platinum-iridium is a compromise wire which does not oxidize. Also, it has better strength that platinum but lower temperature coefficient of resistance.

These wires have been used since 1950 (Sandborn, 1972), most probably long before that. Any of them cannot be said to be the best for all applications, but tungsten is used more commonly than other materials.

As it will be investigated following sections, dimensions of sensor affect directly flow measurements and come into play. For examples, with respect to length:

1. A short sensor is desired to:
    - Maximize spatial resolution
    - Minimize aerodynamic stress
2. A long sensor is desired to:
    - Minimize conduction losses to supports
    - Provide a more uniform temperature distribution
    - Minimize support interference

And, with respect to diameter:

1. A small diameter is desired to:
    - Reduce output noise by reason of separated flow around the sensor
    - Maximize the time response of the wire due to low thermal inertia and higher heat transfer coefficient
    - Maximize spatial resolution
    - Improve the signal-to-noise ratio at high frequencies
2. A large diameter is desired to:
    - Increase strength
    - Reduce contamination effects due to particles in the fluid.

1.5. Anemometer Types

There are three methods of measuring flow velocity using an anemometer bridge combination namely:

I. Constant Current Method
II. Constant Temperature Method
III. Constant Voltage Method

The Constant Voltage Anemometer (CVA) is a new type hot-wire anemometer specifically designed for high-performance flow measurements and is under developing. Thus, it will not be explained in this study.

1.5.1. **Constant Current Method**

The bridge arrangement along with the Constant Current (CC) circuit has been shown in Figure1.8.

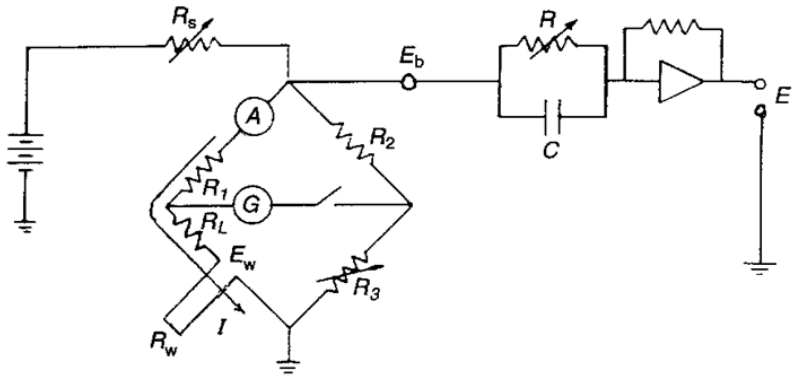

Figure1.8. A typical CC circuit.
(Source: Bruun, 1996)

A constant current is passed through the sensing wire and therefore, the wire is heated. That is, the voltage across the bridge circuit is kept constant. Due the fluid flow, heat transfer takes place from the wire to the fluid and hence the temperature of the wire decreases causing a change in the resistance of the wire. Due to this, galvanometer which was initially at zero position deflects and this deflection of the galvanometer gives a measure of flow velocity.

Although Constant Current Anemometry (CCA) has higher frequency response, there are few disadvantages. This method is difficult to us, because constant temperature anemometry is used the same way as it is calibrated. Calibration is dynamic in this case, while in CCA instruments is calibrated at constant temperature and used in a constant current mode. In constant current mode, wire can be destroyed by burning out due to critical heat flux if the velocity is very small.

1.5.2. **Constant Temperature Method**

The bridge arrangement along with the Constant Temperature Anemometer (CTA) circuit has been shown in Figure 1.9. The temperature of the filament wire is kept constant in this arrangement so its name implies.

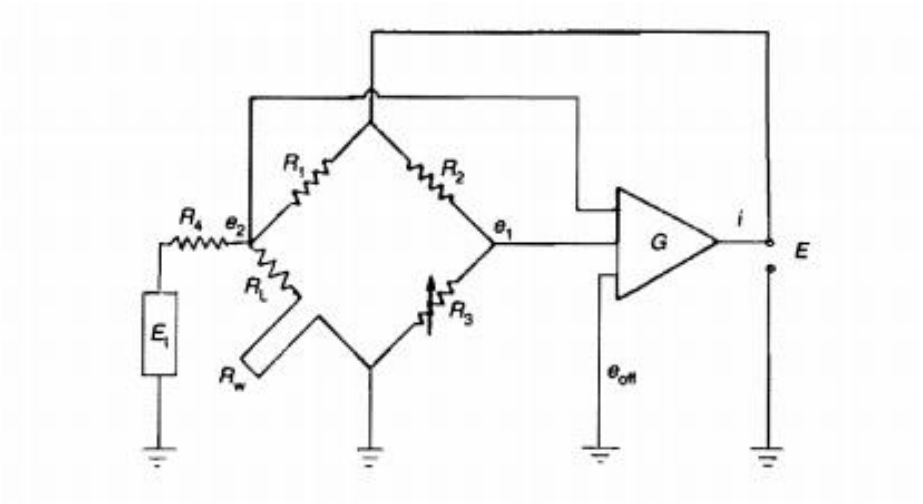

Figure 1.9. A typical CT circuit.
(Source: Bruun, 1996)

This circuit is Wheatstone bridge with an Op-Amp (operational amplifier) and an adjustable resistor. A current passed through the wire heats it up. Due to fluid flow, convective heat transfer takes place from the sensing wire and this decrease the temperature and hence the resistance of wire. The principle in this method is to maintain the temperature and therefore, the resistance of the heated wire at a constant level. Therefore, along with cooling effect, the current through the heated wire is increased by using servo amplifier to bring the sensing wire to have its initial resistance and temperature.

Nowadays, CT method has become standard electronic system for fluid flow measurements.

1.6. Control Circuit

Use of constant temperature systems has increased since about 1960, associated with both improved electronic technology and understanding of the system's characteristics. Therefore, in the following, only constant temperature circuit is explained.

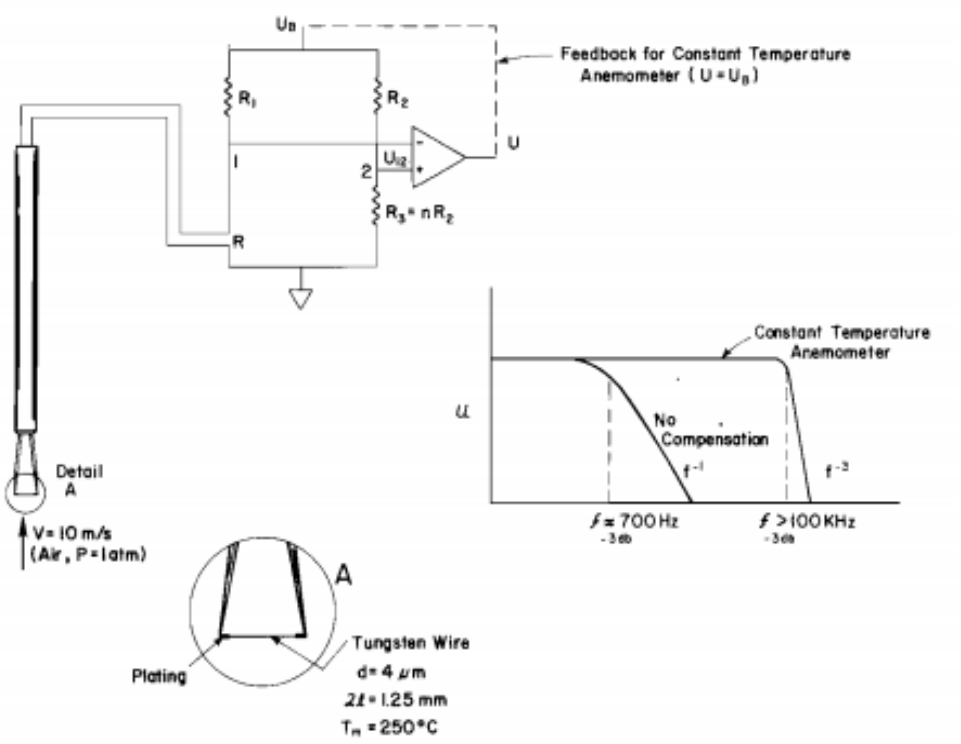

Figure 1.10. Basic elements of a hot-wire anemometer.
(Source: Goldstein, 1996)

Figure 1.10 shows a very basic control circuit for heated wire. Adding a feedback line converts the bridge circuit and amplifier to a constant temperature system, aka servo amplifier. Operation is expressed step by step as follows (Goldstein, 1996):

1. Velocity increase past the heated wire cools it, lowering the temperature, the resistance R, and the voltage at point 1.
2. The lowered voltage at the negative input to the amplifier causes the voltage U_{12} to increase.
3. The increased amplifier input voltage U_{12} increases the output voltage of the amplifier U.
4. The increased voltage on the bridge U increases the current through the sensor.
5. The increased current heats the sensor, resulting in a decrease in U_{12} until the entire system is again in equilibrium.

   All these steps are performed sequentially.

1.7. Calibration of a HWA

A typical static calibration curve for a hot-wire is shown in Figure 1.11.

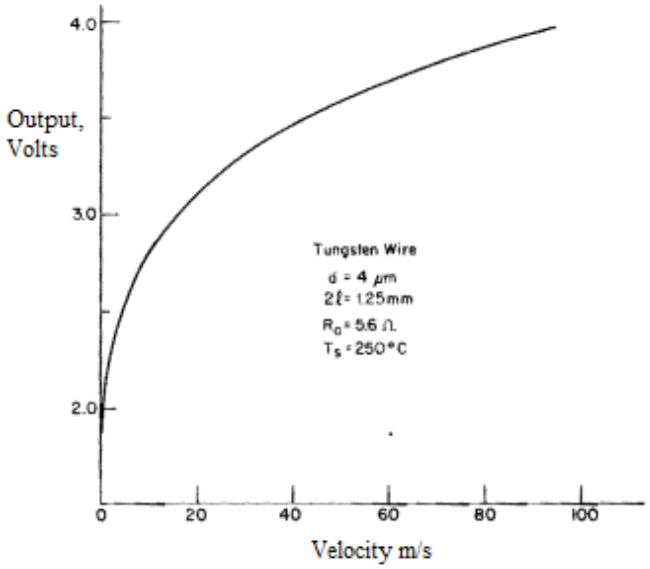

Figure 1.11. Typical static calibration curve for a hot-wire anemometer. (Source: Goldstein, 1996)

According to Figure 1.11, it can be deduced as:

- The output is very non-linear with velocity.
- Sensitivity, $\frac{\partial E}{\partial U}$ decreases as velocity increases.

Calibration system of HWA is basically given in Figure 1.12.

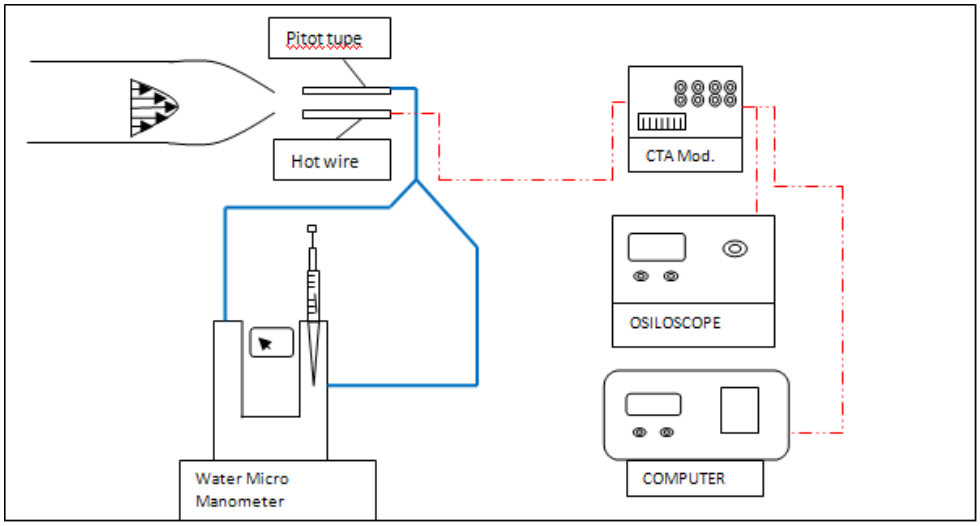

Figure 1.12. Typical calibration system for a hot-wire anemometer.

It is called static calibration because of applied under uniform velocity condition. And, hot-wire system gives a very quick response to measure flow velocity. However, hot-wire is used for turbulent measurements and velocity has not only uniform part, but also fluctuations part. Therefore, it would seem to be needed dynamic calibration. But, it is assumed that if any change occurs in flow velocity (fluctuations), static calibration will include fluctuations due to its good frequency response.

By measuring the total pressure upstream by using pitot tube and manometer which are shown in Figure 1.12, the velocity in the nozzle can be easily calculated with simple relation:

$$V = \sqrt{2\ g\ h_t} \tag{1.1}$$

where g is gravitational constant and h_t is total pressure in height of fluid flowing.

The hot-wire responds according to King's Law (King, 1914):

$$E^2 = A + BV^n \tag{1.2}$$

where E is the voltage across the wire, V is the velocity of the flow normal to the wire and A, B and n are constants. A and B can be found by measuring the voltage, E, obtained for number of known flow velocities and performing one of the fitting methods for the values of A and B which produce the best fit to data. The values of A and B depend on the settings of the anemometer circuitry, the resistance of the wire, the air temperature and the relative humidity of the air and affect calibration curve.

To obtain calibration curve similar to Figure 1.11, listed conditions must be fulfilled (Goldstein, 1996).

1. The fluid temperature, composition and density in the unknown environment are the same as those during calibration.
2. The turbulence intensity is below 20%.
3. The flow is incompressible.

Once these requirements are satisfied, the single sensor hot-wire can be used for measuring mean velocity, turbulence intensity, turbulence spectrum, waveform and flow transients. This is achieved with converting voltage to velocity by use of a calibration curve (Arts et al., 1994).

In this thesis, the main aim is to investigate influence of the sensor parameters on behavior of the constant temperature hot-wire anemometer analytically and numerically at varying conditions. Also, some developments have been studied for improving sensitivity (frequency response) and temperature distribution along the heated wire. Most significant part of this study is that dynamic response of hot-wire has been studied at different sensor parameters and operating flow velocities by using perturbation method. Moreover, any heat transfer from the sensor to the supports by conduction is a "loss" and a potential error source for HWA. Therefore, wire with copper-plated ends has been studied to reduce the amount of heat dissipated by the prongs. Also, effect of conduction end losses on dynamic response of hot wire has been investigated. In the following sections, basic principles of heat transfer from heated wire are presented and some similar studies about hot-wire anemometry are evaluated for this study. After that, the obtained results will be compared with previous studies.

CHAPTER 2

THEORY OF OPERATION

This chapter describes the basic principles of heat transfer from heated wire. The heat is generated inside the hot wire by means of Joule heating. Wire losses heat by convection, conduction, and radiation depending on flow condition. Heat-rate balance equation will be investigated for an incremental wire element. After that, steady and time dependent temperature distribution equations of hot-wire element will be derived from heat-rate balance equation.

2.1. Heat Transfer

The total amount of heat transferred from a heated wire exposed to the fluid flow depends on the flow velocity, the difference in temperature between the wire and the fluid, the physical properties of the fluid and the dimensions and physical properties of the wire. Generally the flow velocity and the dimensions and physical properties of the wire are known. If the physical properties of the fluid is known or kept constant, the velocity can be determined; or velocity is known or constant, those properties can be measured.

2.1.1. **Heat-Rate Balance**

Neglecting for the time being any compressibility effect, non-dimensional heat transfer parameters are listed below:

$$Nu = \frac{hd}{k_f} \tag{2.1}$$

$$Pr = \frac{c_p \mu}{k_f} \tag{2.2}$$

$$Re = \frac{\rho U d}{\mu} \tag{2.3}$$

$$Gr = \frac{g\rho^2 d^3 \beta_v (T_w - T_a)}{\mu^2} \tag{2.4}$$

$$Ma = \frac{U}{c} \tag{2.5}$$

where c is speed of sound.

Nusselt number is very crucial parameter on heat transfer process. Therefore, it takes place in the mathematical treatment of heated wire which will be mentioned later. Representative expression for the Nu in terms of the fluid and sensor parameters is shown as (Goldstein, 1996);

$$\mathrm{Nu} = f\left(Re, Pr, \alpha_1, Gr, Ma, \gamma_h, a_T, \frac{2l}{d}, \frac{k_f}{k_w}\right) \tag{2.6}$$

where $\mathrm{Re} = \mathrm{Ud}/\vartheta =$ Reynolds number

U = free stream velocity

$\vartheta =$ kinematic fluid viscosity

μ = dynamic fluid viscosity

$\mathrm{Pr} = \mu C_p/k$ = Prandtl number

$C_p =$ specific heat of fluid at constant pressure

α_1= angle between free-stream flow direction and normal to cylinder

$\mathrm{Gr} = \rho^2 g \beta_v (T_m/T_a)\, d^3/\mu^2$ = Grashof number

$\beta_v = 1/T_a$ = volume coefficient of expansion

$\mathrm{Ma} = V/\gamma_h\, R_0 T_a{}^{1/2}$ = Mach number

$R_0 =$ gas constant

$\gamma_h = C_p/C_v$

C_v = specific heat at constant volume

$a_T = (T_m/T_a)\ /T_a$ = overheat ratio or temperature loading

k_w= thermal conductivity of sensor material

When fluid temperature is kept constant, Prandtl number does not affect Nusselt number. Velocity direction and the wire are taken to be perpendicular in this thesis, hence α_1 is immaterial. It was found (Collis & Williams, 1959) that buoyancy effects (free convection) are valid for only if

$$Gr^{\frac{1}{3}} > Re$$

To investigate energy balance for HWA, it can be taken differential element of small length of the heated wire, as shown in Figure 2.1. The heat which is generated in small differential element is dissipated by convection to the fluid, by radiation to the surroundings and by conduction to any neighboring metals such as the prongs. Moreover, there is a heat accumulation in the differential element of wire. Prongs are massive, and the prong temperature, T_p, can be assumed to be equal to ambient temperature, T_a. Temperature distribution along the heat wire is derived from heat-rate balance equation. Typical temperature distribution and incremental element can be seen in Figure 2.1.

$$d\dot{Q}_e = d\dot{Q}_{fc} + d\dot{Q}_c + d\dot{Q}_r + d\dot{Q}_s \tag{2.7}$$

where $d\dot{Q}_e$ is the electrical heat-generation rate,

$d\dot{Q}_{fc}$ is the forced-convective heat-transfer rate,

$d\dot{Q}_c$ is the conductive heat-transfer rate,

$d\dot{Q}_r$ is the radiation heat-transfer,

$d\dot{Q}_s$ is the heat storage rate.

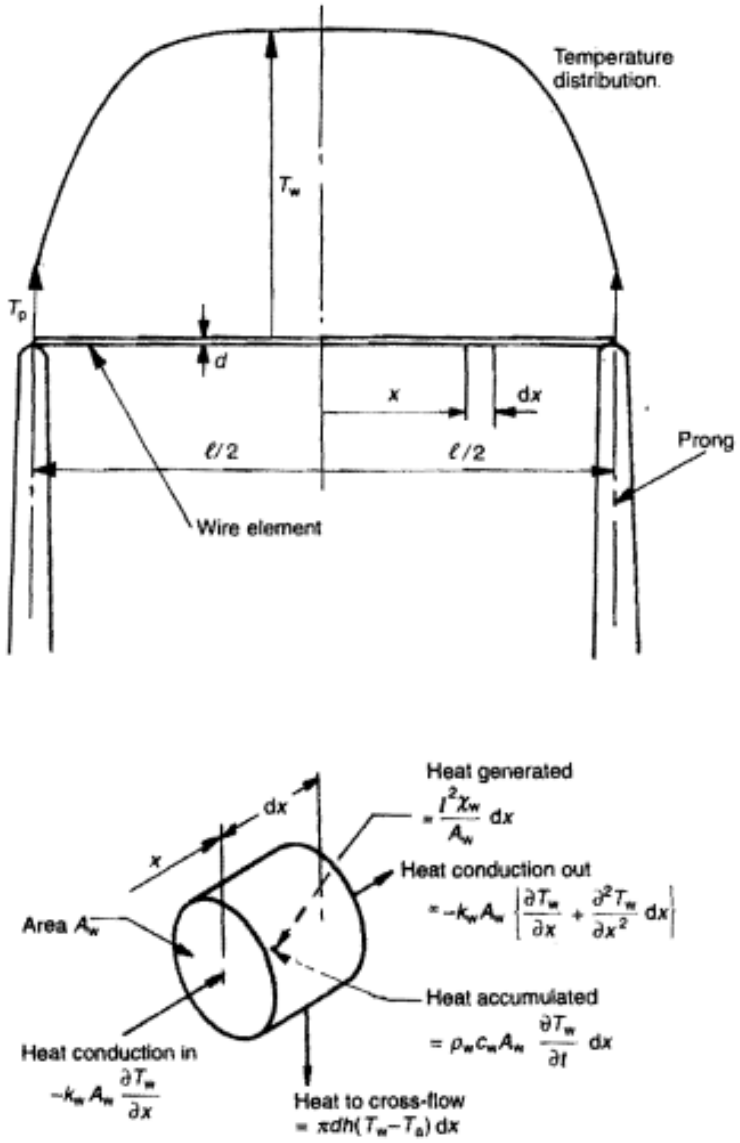

Figure 2.1. The hot-wire geometry and heat balance for an incremental element. (Source: Bruun, 1996)

The rate of heat generation can be calculated as a function of electric current, I, is:

$$d\dot{Q}_e = \frac{I^2 \gamma_w}{A_w} dx \tag{2.8}$$

where γ_w is the electrical resistivity of the probe material and A_w is the cross-sectional area. The rate of forced-convection heat transfer, $d\dot{Q}_{fc}$, to the fluid can be explained in terms of the heat transfer coefficient, h:

$$\mathrm{d}\dot{\mathrm{Q}}_{\mathrm{fc}} = \pi \mathrm{dh}(T_w - T_a)\mathrm{dx} \tag{2.9}$$

where T_w is wire temperature and T_a is ambient temperature. The rate of the overall conduction heat-transfer can be calculated from Fourier law as:

$$d\dot{Q}_c = -k_w A_w \frac{\partial^2 T_w}{\partial x^2} dx \tag{2.10}$$

where k_w is the thermal conductivity of the wire material at the wire temperature, T_w. The heat transfer rate of radiation can be calculated by Stephan-Boltzman law as:

$$d\dot{Q}_r = \pi d\sigma\epsilon\left({T_w}^4 - {T_s}^4\right)dx \tag{2.11}$$

where σ is the Stefan-Boltzmann constant, ϵ is the emissivity of the sensor, and T_s is the temperature of the surroundings. The heat-storage rate is

$$d\dot{Q}_s = \rho_w c_w A_w \frac{\partial T_w}{\partial t} dx \tag{2.12}$$

where ρ_w is the density of the wire material and c_w is the specific heat of the wire material.

Substituting these relations into Equation (2.7) and the following energy balance could be found:

$$\begin{aligned} k_w A_w \frac{\partial^2 T_w}{\partial x^2} + \frac{I^2 \gamma_w}{A_w} - \pi dh(T_w - T_a) + \pi d\sigma\epsilon\left({T_w}^4 - {T_s}^4\right) \\ - \rho_w c_w A_w \frac{\partial T_w}{\partial t} = 0 \end{aligned} \tag{2.13}$$

2.1.2. **Steady-State Temperature Distribution in Heated Wire**

Under steady conditions, temperature is not changing with time; $\frac{\partial T_w}{\partial t} = 0$. The temperature dependence of the resistivity for the heated wire material is in the form

$$\gamma_w = \gamma_a + \gamma_0\, \alpha_0 (T_w - T_a) \tag{2.14}$$

where $\gamma_a$the resistivity is value at ambient fluid temperature, γ_0 is the resistivity value at 0 ℃, and α_0 is the temperature coefficient of resistivity at 0 ℃.

After all, the radiation term which will be investigated next section is very small and it is omitted in most HWA applications (Bruun, 1996). Also, mean value of heat transfer coefficient, h, is assumed to be constant. Then, Equation (2.13) can be rewritten as:

$$k_w A_w \frac{\partial^2 T_w}{\partial x^2} + \left(\frac{I^2 \gamma_0 \, \alpha_0}{A_w} - \pi d h\right)(T_w - T_a) \; + \; \frac{I^2 \gamma_a}{A_w} = 0 \tag{2.15}$$

To simplify Equation (2.27), it can be written as:

$$\frac{\partial^2 T}{\partial x^2} + K_1 \, T \; + \; K_2 = 0 \tag{2.16}$$

where

$$T = \; T_w - T_a \tag{2.17}$$

and

$$K_1 = \frac{I^2 \gamma_0 \, \alpha_0}{k_w {A_w}^2} - \; \frac{\pi d h}{k_w A_w} \tag{2.18}$$

$$K_2 = \frac{I^2 \gamma_a}{k_w {A_w}^2} \tag{2.19}$$

The solution for second order homogeneous differential equation becomes (Bruun, 1996)

$$T_w = \; \frac{K_2}{|K_1|}\left[1 - \frac{\cosh(|K_1|^{1/2} \, x)}{\cosh(|K_1|^{1/2} \, l/2)}\right] + T_a \tag{2.20}$$

Equation (2.20) shows the temperature variation along its length. Constant temperature anemometer provides mean wire temperature constant. Mean wire temperature, $T_{w,m}$ is then expressed as:

$$T_{w,m} = \frac{1}{l}\int_{-l/2}^{l/2} T_w(x)dx \tag{2.21}$$

Non-dimensional steady state temperature distribution along the heated wire can be obtained with using Equation (2.20) and (2.21) by computer program.

$$\frac{T_w - T_a}{T_{w,m} - T_a} = \frac{1 - \cosh\left(|K_1|^{1/2}\, x\right)\operatorname{sech}(|K_1|^{1/2}\, l/2)}{1 - \dfrac{2\tanh(|K_1|^{1/2}\, l/2)}{|K_1|^{1/2}\, l}} \tag{2.22}$$

All things considered, it is useful to think heat transfer from the sensor to its environment as the key point. Mainly, the heat transfer consists of two parts and equals to Joule power:

1. Convective heat transfer $\dot{Q}_{fc}$ between the heated part of the sensor and the fluid.
2. Conduction heat transfer $\dot{Q}_c$ between the heated part of the sensor and its supports. This heat $\dot{Q}_c$ is usually moved into the following fluid by convection

$$\mathrm{H} = \mathrm{P} = \dot{Q}_{fc} + \dot{Q}_c \tag{2.23}$$

H = heat transfer from sensor to environment

P = electric power input to sensor

The conductive heat loss, $\dot{Q}_{cp}$which is between supports and heated wire breaks the uniformity of temperature distribution. Also, it can be called error for measurement because pure convective heat transfer will give maximum accuracy.

$$\dot{Q}_{cp} = 2\, k_w A_w \left|\frac{\partial T_w}{\partial x}\right|_{x=l/2} \tag{2.24}$$

After that, convective heat transfer along the wire can be defined as according to the Equation (2.9):

$$\dot{Q}_{fc} = \int_{-l/2}^{l/2} \pi dh\,(T_w - T_a)\,dx \tag{2.25}$$

Minimizing conduction losses provides more precision for making good measurements. To achieve this, the ratio of conduction to convection heat transfer should be as low as possible. This ratio is shown in Equation (2.26).

$$\frac{\dot{Q}_{cp}}{\dot{Q}_{fc}} = \frac{2\,A_w k_w |K_1| \tanh\left(|K_1|^{1/2}\, l/2\right)}{d\,h\,\pi\,(|K_1|^{1/2}\, l - 2\tanh(|K_1|^{1/2}\, l/2))} \tag{2.26}$$

If required improvements are applied for minimizing end losses, conduction term can be ignored. Then, the heat-transfer relationship can be expressed for a finite long wire with in steady state temperature distribution ($\frac{\partial T_w}{\partial t}$=0), and the heat balance can be written to the wire of l by using Equation (2.13)

$$I^2 R_w = \pi dhl(T_w - T_a) = \pi l k_f (T_w - T_a) Nu \tag{2.27}$$

By introducing the $E_w = I\,R_w$, new form of the Equation (2.27) is

$$\frac{{E_w}^2}{R_w} = \pi l k_f (T_w - T_a) Nu \tag{2.28}$$

There are many investigations about expression of Nusselt number. Main purpose of those investigations is giving general and practical expression. The simplest form of the Nusselt number was built by King (1914) and called as "King' Law" (King, 1914):

$$\mathrm{Nu} = \mathrm{A}' + \mathrm{B}'(\mathrm{Re})^{\mathrm{n}} \tag{2.29}$$

where A' and B' are empirical constants.

Equation (2.29) is still using in lots of thermal anemometry applications because of its simplicity. But investigations show that it does not give accurate results for wide range of velocities. Collis & Williams (1959) was found much more accurate expression for air:

$$\mathrm{Nu} = (\mathrm{A} + \mathrm{B}(\mathrm{Re})^{\mathrm{n}}) \left(1 + \frac{a_T}{2}\right)^{0.17} \tag{2.30}$$

where

A=0.24	B=0.56	n=0.45	for	0.02 < Re < 44
A=0	B=0.48	n=0.51	for	44 < Re < 140

Relationship between analog voltage and velocity is achieved with using Nusselt expression and Equation (2.28). In this study, Re is 0.576 for most of the cases.

CHAPTER 3

LITERATURE SURVEY

Hot-wire anemometers have been used for a long time. The exact origin of hot-wire anemometry cannot be known strictly but it seems to go back to the beginning of the last century. According to King (1915), some experiments with heated platinum wire were carried out to measure wind velocity by Shakespeare, at Birmingham, but they were discontinued because of lack of facilities for calibration process. Earlier investigations considered only the mean heat transfer characteristics from heated wire and it was significant for the design of hot-wire anemometers and understanding heat transfer over the cylindrical wire.

One of the analytical investigations about heat transfer of hot-wire anemometry was done by Manshadi & Esfeh (2012). In this study, the sensing element is a standard 5 μm tungsten wire which is heated by an electric current to a temperature of 250 °C. The active wire length is 1.25 mm. To study the behavior of the hot-wire sensor in different conditions, the energy balance equation was firstly built up. They assumed that there is the uniform temperature over the heated wire.

$$\frac{I^2\gamma_w}{A_w} = -k_w A_w \frac{\partial^2 T_w}{\partial x^2} + \pi d h (T_w - T_a) + \pi d \sigma \varepsilon \left({T_w}^4 - {T_s}^4\right) + \rho_w c_w A_w \frac{\partial T_w}{\partial t} \tag{3.1}$$

In the beginning of the study, they studied whether radiation term is important or not. With using the fourth-order Runge-Kutta method, this non-linear secondary differential equation is solved in two conditions: with radiation term and without radiation term. Figure 3.1 shows that radiation term does not have any effect on the temperature distribution.

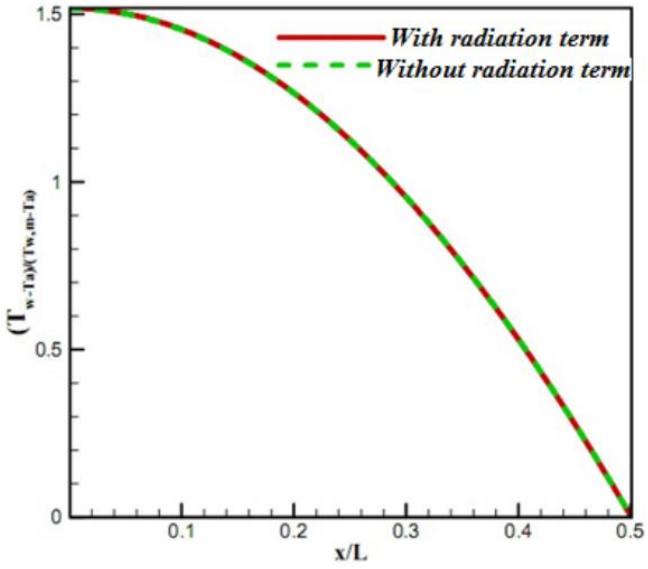

Figure 3.1. Solution of energy balance equation with and without radiation term.
(Source: Manshadi & Esfeh, 2012)

After neglecting radiation term, they investigated effect of diameter and length of wire on temperature distribution and percent of conductive and convective heat transfer. Figure 3.2 shows that temperature distribution becomes more uniform with increasing length of wire. Also, their work shows that conduction end losses are reduced with increasing the wire length in Figure 3.3. After that, effect of wire diameter on the temperature distribution along the heated wire is shown in Figure 3.4. As it is shown, diameter is more important parameter than wire length on the temperature distribution.

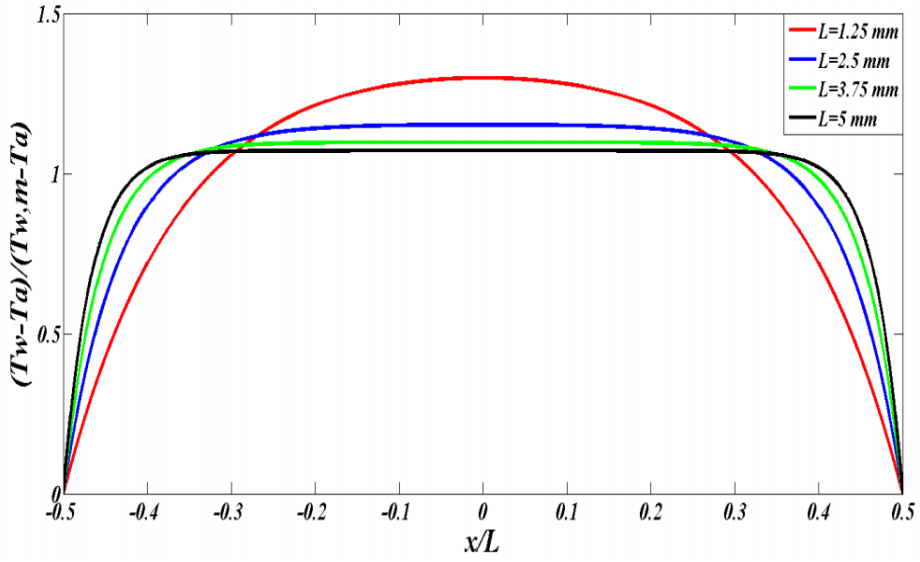

Figure 3.2. Temperature distribution with various lengths.
(Source: Manshadi & Esfeh, 2012)

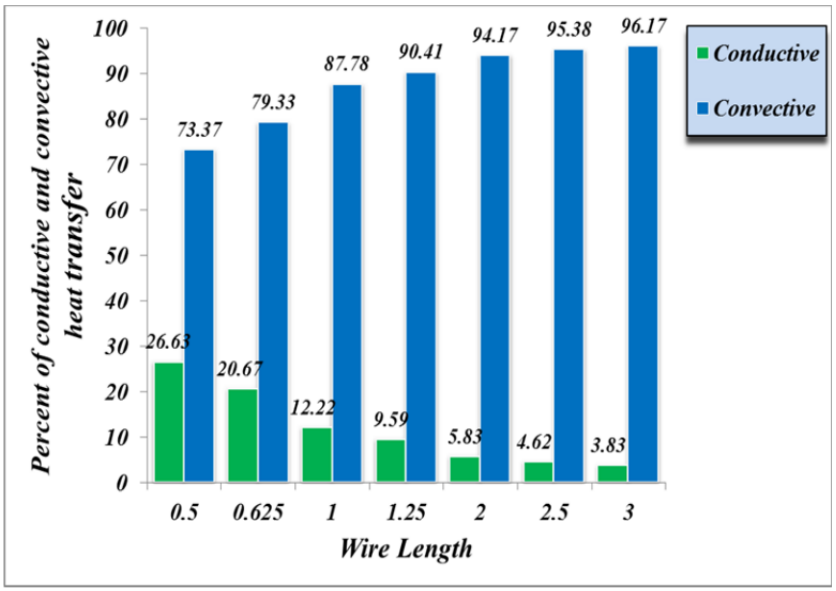

Figure 3.3. The percent of conduction and convection heat transfer for various lengths. (Source: Manshadi & Esfeh, 2012)

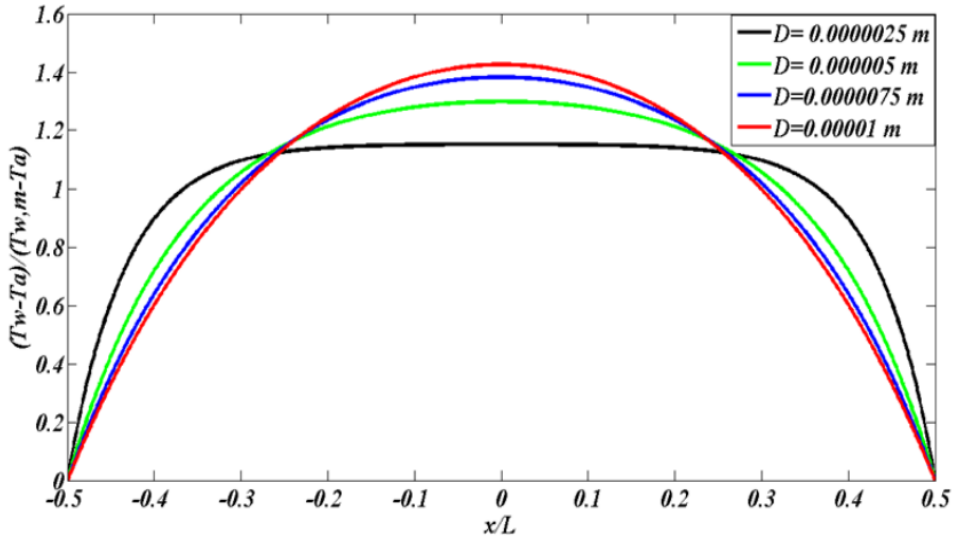

Figure 3.4. Temperature distribution with various diameters (Source: (Manshadi & Esfeh, 2012))

Manshadi & Esfeh (2012) also mentioned that convective heat transfer is the most dominant parameter for principle of hot-wire anemometer, since the heat transfer is directly proportional to the temperature difference between the sensor and the fluid. Therefore, ambient temperature variations are one of the significant error sources in the measurements with the hot-wire anemometer. It can be seen in Figure 3.5, the achieved results indicate convection heat transfer coefficient and Nusselt number vary with variation of air flow temperature. If it is desired to obtain precise results, experimental

conditions must be kept constant or new compensation techniques should be studied. So, they have studied about compensating for the ambient temperature variations in "New Approach about Heat Transfer of Hot-Wire Anemometer" (Mojtaba Dehghan Manshadi, 2012).

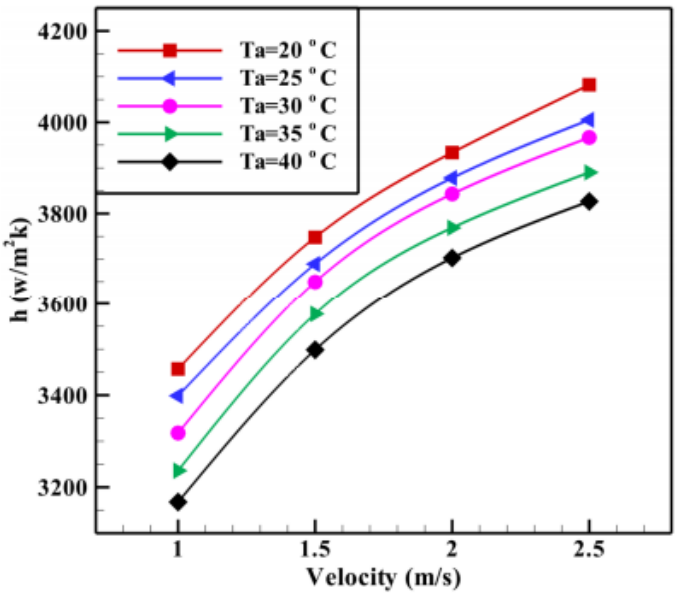

Figure 3.5 Variation of heat transfer coefficient at different ambient temperatures (Source: Mojtaba Dehghan Manshadi, 2012)

The other important study on the convective heat transfer from circular cylinders was done by A. Al-Salaymeh (2005). This work includes analytical and numerical investigation of single hot-wire to study the parametric effect on the accuracy of hot-wire anemometry. He solved the second order partial differential equation (energy balance equation) numerically by using finite element method. This study shows that non-uniform temperature distribution exists along hot-wire due to the cooling effect of prongs (conduction end losses) as it shown in Figure 3.6. And, it has been found that the effect of conduction end loses through the prongs is negligible if the aspect ratio (L/d) is larger than 250 (see Figure 3.7). Therefore, this study says that if it is desired to produce a uniform temperature distribution, high aspect ratios is recommended in order to reduce conduction heat losses and to get uniform temperature distribution along the hot-wire. Moreover, it was shown that the percentage of radiation from the total heat losses does not exceed 0.2%, because of this reason it can be neglected. Also, the sensitivity of hot-wire has discussed in his study. The sensitivity of hot-wire is high at low velocities and it is low at very high flow velocities.

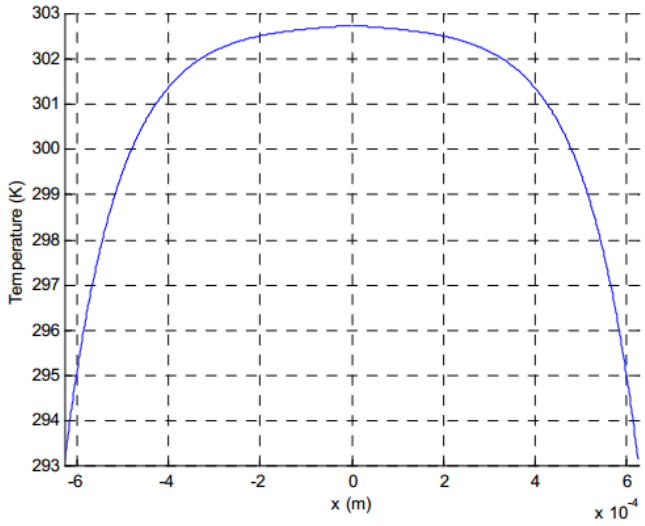

Figure 3.6. Temperature distribution along the hot-wire.
(Source: Al-Salaymeh, 2005)

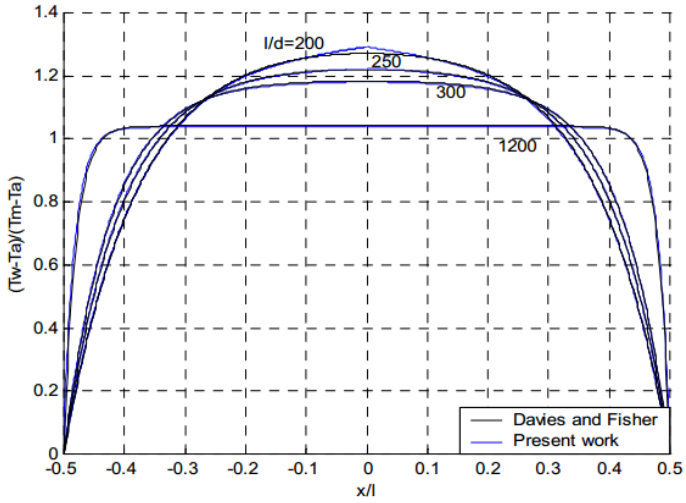

Figure 3.7. A comparison of the present results for temperature distributions along the hot-wire for different aspect ratios and the results of Davies and Fisher work. (Source: Al-Salaymeh, 2005)

The dynamic response of the heated wire has been investigated by Freymuth (1979), Hinze (1975) and Perry (1982) analytically. Perry (1982) analyzed the dynamic response of the heated wire by using perturbation in velocity, temperature and electrical current separately. Hinze (1975) analyzed the dynamic response of the heated wire by putting perturbations into the electrical resistance. However, J D Li (2004) mentioned that the fluctuations in the output voltage depends only the velocity fluctuations over the wire and the resistance fluctuations can only be a consequence of this velocity variation.

Li (2004) studied dynamic response of CTA in turbulence velocity measurements. In this paper, analytical solution for the temperature fluctuations over the heated wire was derived for turbulent velocity fluctuations. Attenuation in frequency response was investigated. By using this solution, effects of different length to diameter ratios, Reynolds numbers, hot-wire materials and overheat ratios was examined.

Some figures from Li's investigation are given in Figure 3.8 to Figure 3.11 and here the physical meaning of ϵ_1 is the same as the ϵ_1' used in Freymuth (1979) for the attenuation which is related to the heat conduction from the hot-wire to its prongs. Actually, amount of attenuation is $1-\epsilon_1$. Figure 3.8 shows that the attenuation is reduced with increasing length to diameter ratio. Since, as the length to diameter ratio increases, conduction end losses becomes relatively less than those of from convection; and therefore, the attenuation gets smaller. Also this figure shows that a higher overheat ratio gives less attenuation.

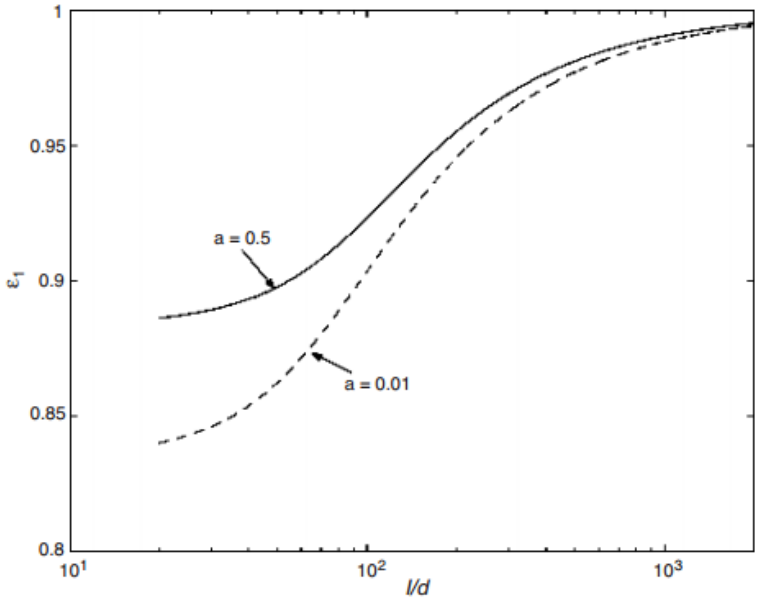

Figure 3.8. The dependence of attenuation on hot-wire length to diameter ratio. (Source: Li, 2004)

Figure 3.9 shows that Reynolds number is inversely proportional to the attenuation. This is because, when the Reynolds number increases, the convective heat transfer becomes more dominant and this causes smaller conductive heat losses.

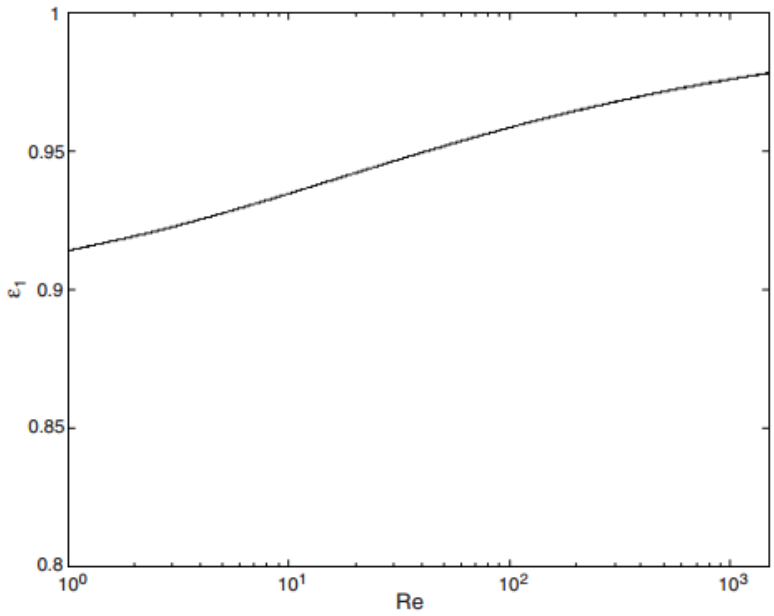

Figure 3.9. The dependence of hot-wire attenuation on Reynolds number.
(Source: Li, 2004)

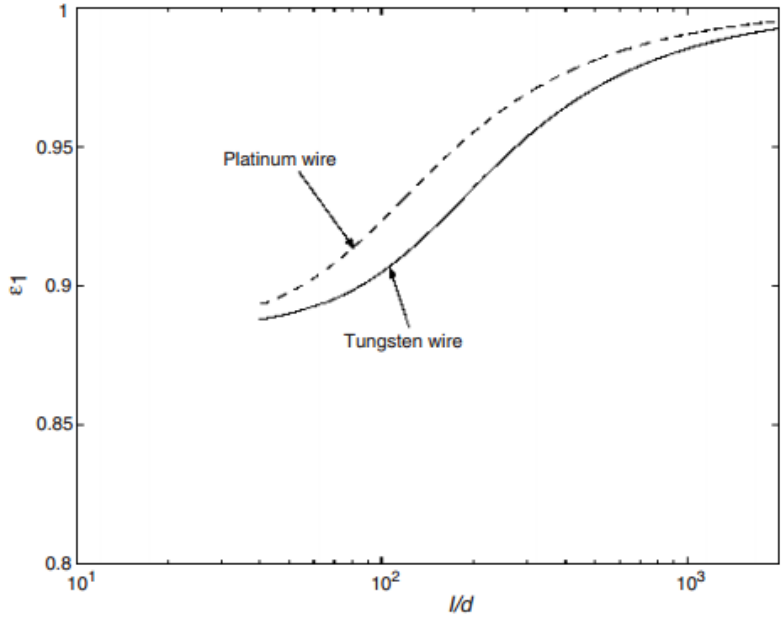

Figure 3.10. Hot-wire attenuation of platinum and tungsten wires.
(Source: Li, 2004)

Figure 3.10 shows that platinum wire gives less attenuation than tungsten wires due to fact that tungsten has higher thermal conductivity. Because of this reason, heat loss from end conduction for tungsten is higher than the platinum at given Reynolds number. However, thermal diffusivity of platinum is lower than that of tungsten. This value describes how quickly a material reacts to a change in temperature. This causes

that the frequency where the tungsten wire begins to attenuate the velocity fluctuations is higher than the platinum for a same aspect ratio. This situation can be seen in Figure 3.11 clearly.

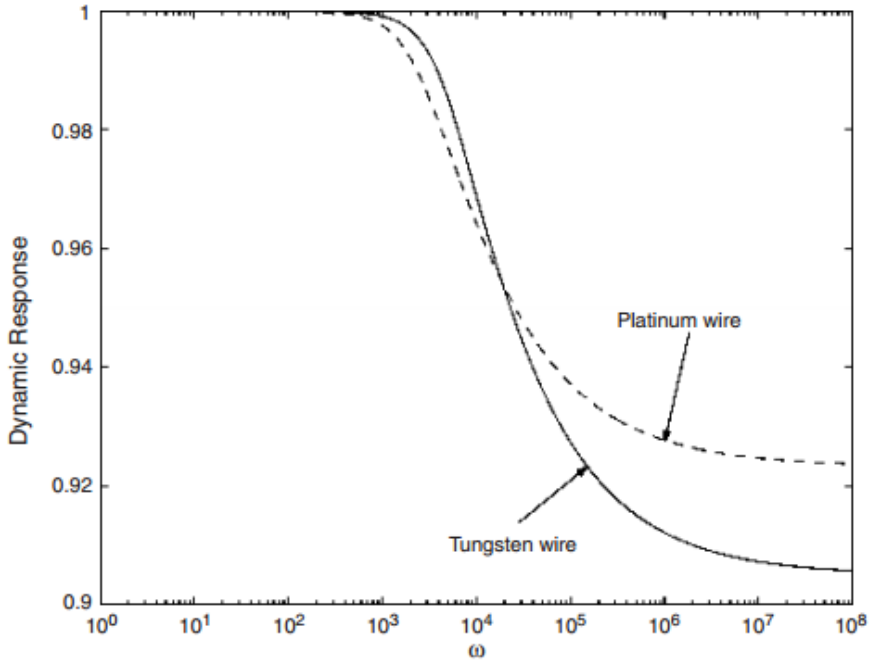

Figure 3.11. Dynamic response of platinum and tungsten hot-wires.
(Source: Li, 2004)

Soe Minn Khine *et al.* (2013) have developed theoretical expression for the frequency response of the constant-current hot-wire anemometer (CCA) and verified its effectiveness experimentally for hot-wires of 5 μm, 10 μm, and 20 μm in diameter. They decomposed the relevant physical properties into a time-averaged component and a fluctuation one as $T = \bar{T} + t,\ h = \bar{h} + h,\ I = \bar{I} + i.$ Also, they have tried compensation techniques on power spectrum. To estimate theoretically the frequency response of heated wire, they have applied their expression to the three different tungsten hot-wires (5 μm, 10 μm, 20 μm in diameter) with copper plated ends. The geometric parameters are given in Table 3.1. All the wires have copper-plated ends 35 um in diameter.

Table 3.1.Detailed features of three different hot-wires used. Definitions of geometrical parameters are given Figure 3.12.

Material	d_1 [μm]	l [mm]	l/d_1	L [mm]
Tungsten	5	1.5	300	5
Tungsten	10	2.0	200	6
Tungsten	20	4.0	200	7

As shown in Figure 3.13, frequency response can be improved by decreasing the wire diameter. Aspect ratios are varied from 200 to 300. In this sense, Hinze (1975) showed that for platinum-iridium wires, the aspect ratio should be higher than 200, and be greater for tungsten wires. Also, they mentioned that if the aspect ratio becomes smaller than 200, the cooling effects of the wire supports will emerge and the frequency response will fall to the lower level.

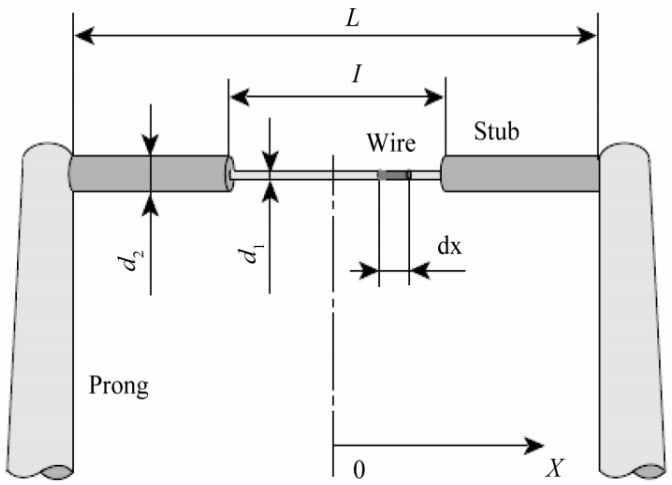

Figure 3.12. Geometric features of hot-wire sensor.
(Source: Soe Minn Khine, 2013)

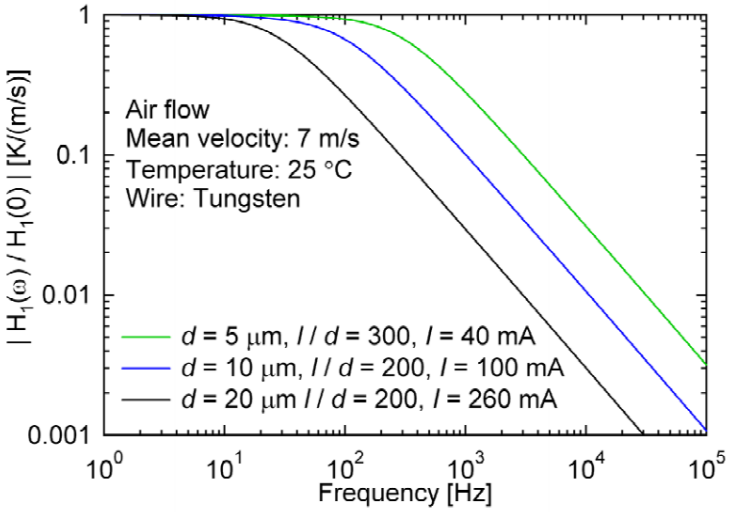

Figure 3.13. Frequency response of CCA.
(Source: Soe Minn Khine, 2013)

Frequency response is investigated as a function of the wire length. As seen from Figure 3.14(a), gain rises with increasing wire length. Also, they mentioned that the heat loss due to conduction becomes higher when the wire length decreases. By this way, conduction becomes an important error source for measurement. Figure 3.14(b) and 3.14(c) show the normalized values as frequency approaches f=0 Hz. Normalized values of frequency response show that short wire has broader frequency response. Therefore, a uniform frequency response gives more sensitivity over the range of interest. It can be concluded that uniformity of frequency response is more significant that gain value.

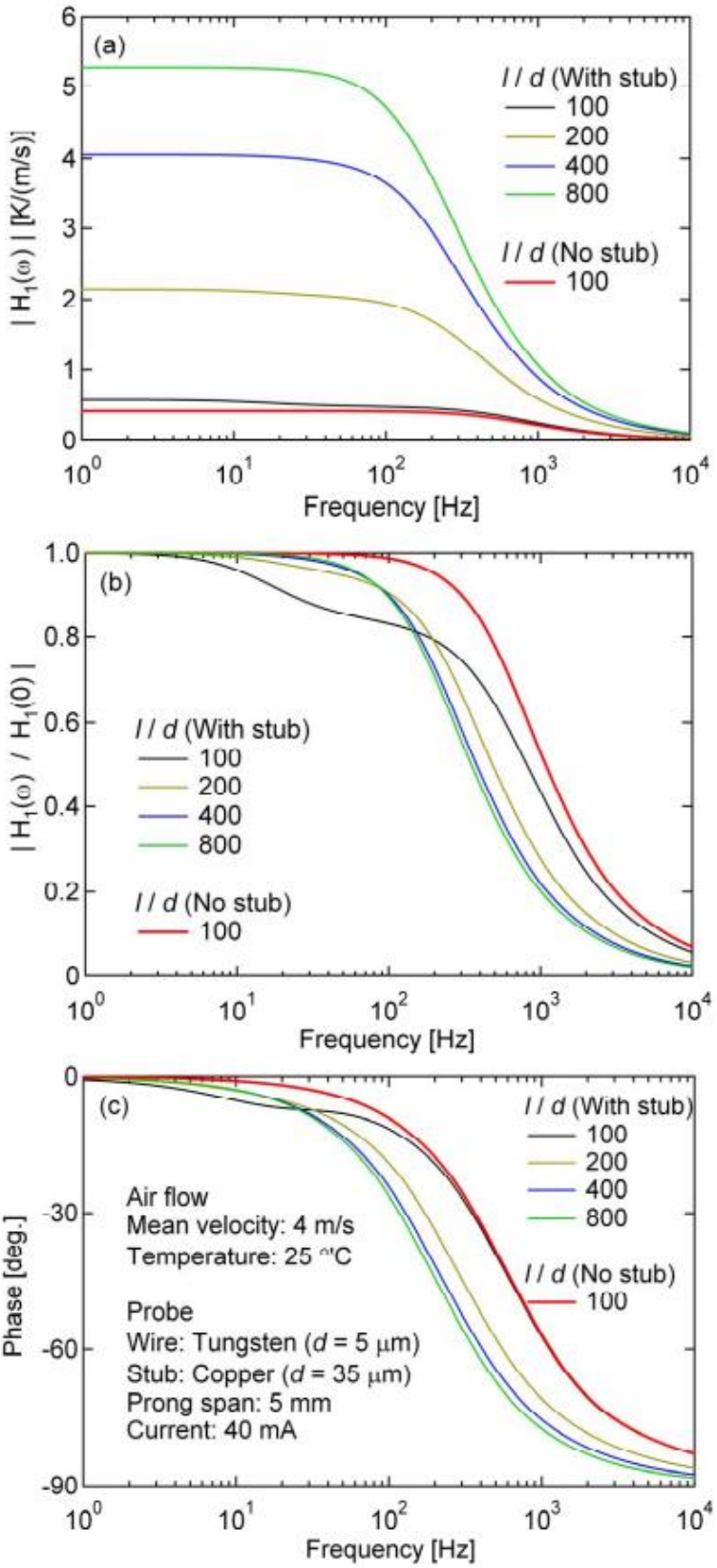

Figure 3.14. Frequency response of CCA: (a) Absolute gain; (b) Normalized gain; (c) Phase Source. (Source: Soe Minn Khine, 2013)

The effect of the thermal transients on the frequency response of the sensor was studied analytically by Freymuth (1979). His equations describe a critical frequency: f_l, above which the sensor response is decreased to a constant value: ϵ_l (see Figure 3.15). The theory provides estimates of ϵ_l and f_l based on the geometric parameter and material properties of the heated wire. This is also confirmed by numerically by Morris and Foss (2013) and analytically by Li (2004).

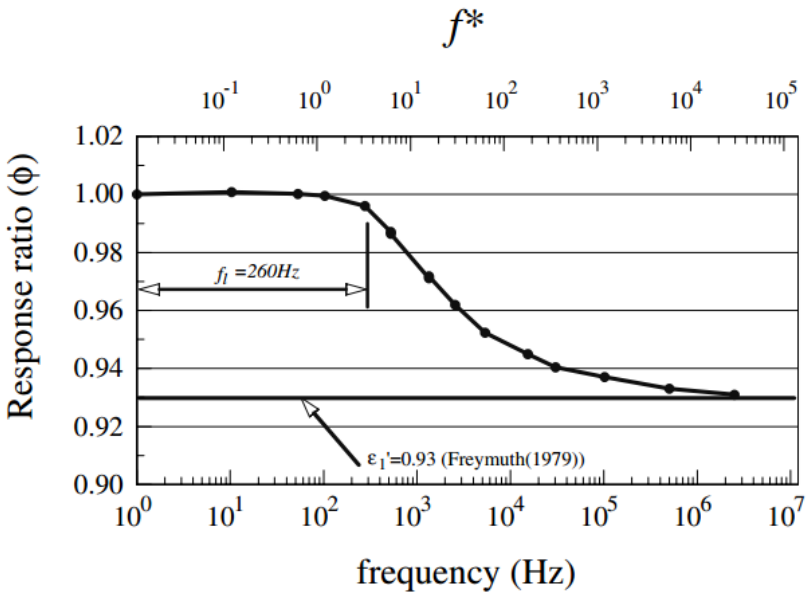

Figure 3.15. Thermal frequency response of Freymuth (1979).
(Source: Morris & Foss, 2003)

Morris and Foss (2013) investigated numerically the effects of thermal transients on the output of the hot-wire system. A typical 5 μm diameter, 1 mm long, tungsten wire was modelled with 50 μm copper plated support stubs. The unplated tungsten was referred as the active portion of the sensor (see Figure 3.16). The half-sensor was discretized with 150 nodes in the tungsten and 15 nodes in the copper plated end. The differential equation governing the transport of thermal energy is same energy balance equation as mentioned before. The time derivative was discretized using a simple forward difference and the conductive heat transfer along the length of the sensor was modelled with a second order spatial difference. Then the frequency response of the sensor was determined by testing a range of sine wave input functions. They deduced that the ability of hot-wire anemometer depends not only the electronic system but also the thermal characteristics of the hot-wire sensor.

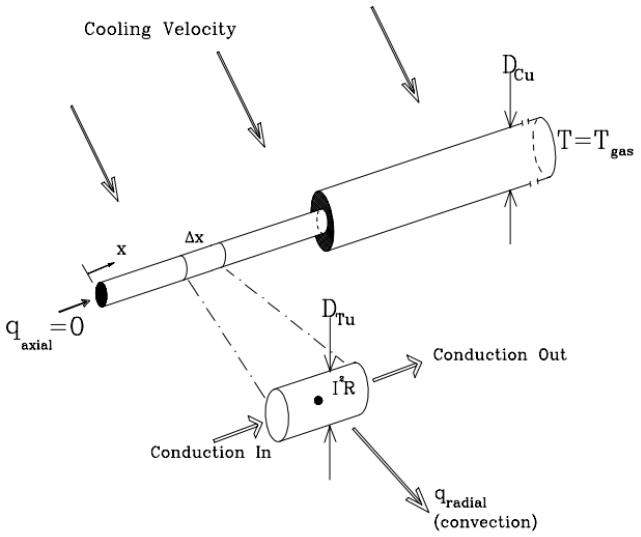

Figure 3.16. Modelled hot-wire (not to scale).
(Source: Morris & Foss, 2003)

One of the most important investigations for dynamic theory of constant temperature operation was done by Beljaars in 1976. The time dependent differential equation is solved for the local wire temperature of a constant temperature anemometer by using straight forward perturbation method. Investigator used harmonically changing heat transfer coefficient for an input and evaluated the influence of thin supporting wires, or copper-plated ends. de Haan (1971) treated the same problem in a different way and achieved at comparable results. Numerical results given below for different cases are of practical interest. Average wire temperature is kept constant at 180 K and velocity is 6 m/s. The amplitude of g_1 is a measure of sensitivity of the wire.

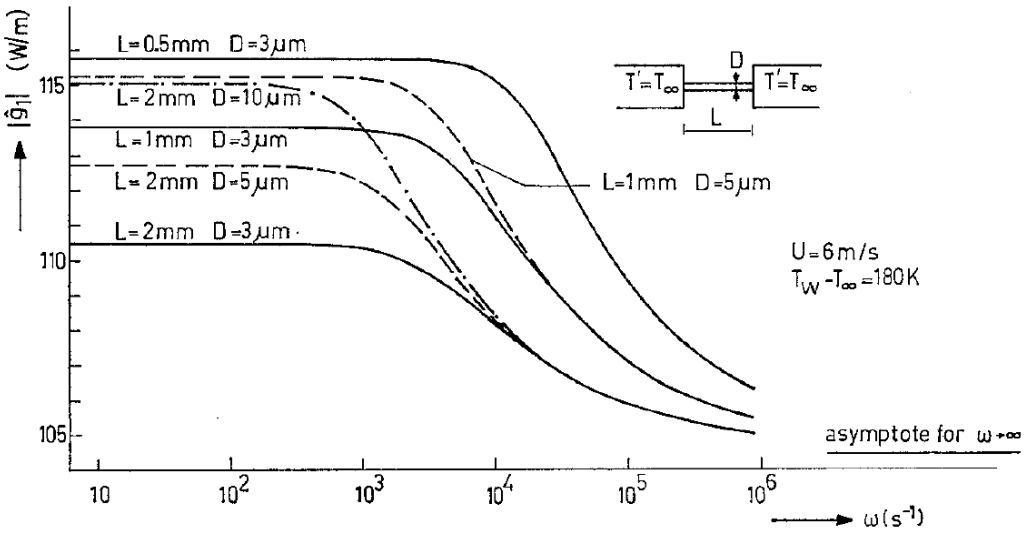

Figure 3.17. Frequency characteristic of hot-wire for various values of *L*and *D*.
(Source: Beljaars, 1976)

Figure 3.17 shows the amplitude characteristics $|g_1|$ which depends on circular frequency, ω. As it can be seen, sensitivity increases with decreasing length and increasing diameter. Moreover, investigator talked about that the deviation of the flat characteristic occurred at characteristic frequency, which is of the order of $1/\tau$, where $\tau = \rho\, c\, D/4\, h$ is the time constant for constant-current operation. After that, he investigated effect of second amplitude, $|g_2|$. The conclusion was that a fist order calculation is enough for very high turbulent intensities. Up to now, it is assumed that ends of wire are equal to ambient temperature. As mentioned before, the temperature distribution will not be uniform as the result of conduction to the prongs. To reduce conduction losses to prongs, wire ends should be plated with copper. The influence of copper-plated ends was evaluated also in his work.

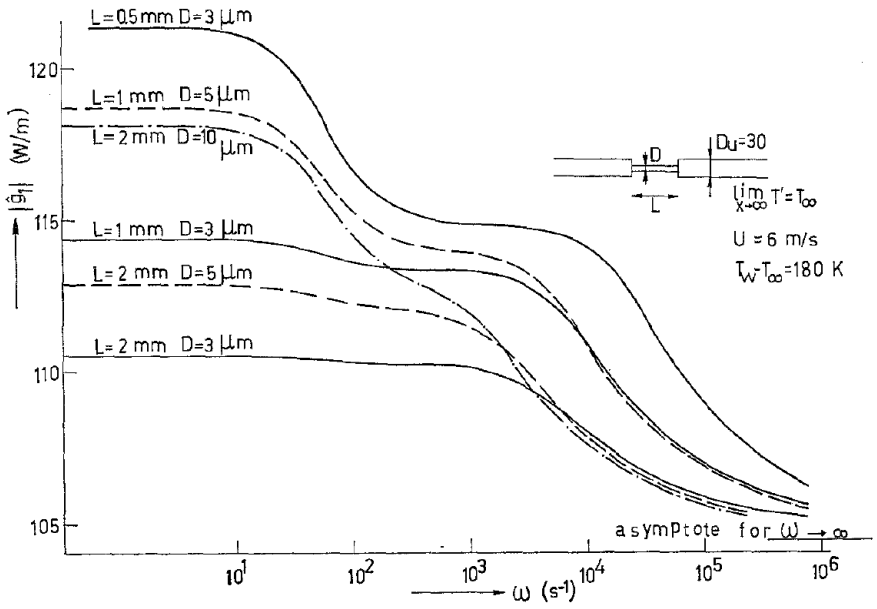

Figure 3.18. Frequency characteristic of hot-wire with copper-plated ends for various values of $L$and D. (Source Beljaars, 1976)

Some frequency characteristics were investigated (see Figure 3.18). Now, frequency response exhibits two steps. The first step is corresponding to the frequency $1/\tau_u$ where τ_u is the time constant for copper-plated wire, the second step is corresponding to that of Figure 3.17. Results give that when diameter of plated end increases, the first step decreases and appears at a lower frequency. It can be concluded that large length-diameter ratio gives better results in order to avoid the effect of thermal inertia of the measuring wire and supporting wires.

CHAPTER 4

PERTURBATION THEORY IN HEAT TRANSFER

Many physics and engineering problems can be modelled by differential equations. However, it is difficult to obtain closed-form solutions for them, especially if they have non-linear form. Perturbation theory helps us to find approximate solutions to a differential equation which otherwise unsolvable. Applying perturbation theory on hot-wire operation is one of the most significant part of this study.

4.1. Perturbation Method

Bender and Orszag (1999) said that *"Perturbation theory is a collection of methods for the analysis of the global behavior of solutions to differential and difference equations"*. In general, the perturbation is valid for weakly non-linear problems (Nayfeh, 2008).

The general procedure of perturbation theory is to identify a small parameter, ε, and study by a local analysis about $\varepsilon = 0$. Thus, a perturbative solution is constructed by local analysis about $\varepsilon = 0$ as series of power which is called straightforward expansion.

$$y = y_0 + \varepsilon\, y_1(x) + \varepsilon^2 y_2(x) + \cdots \tag{4.1}$$

Initial value problem can be handled as an example for straightforward expansion.

$$y'' = f(x)y, \qquad y(0) = 1, \qquad y'(0) = 1 \tag{4.2}$$

First, ε is introduced into the problem:

$$y'' = \varepsilon\, f(x)y, \qquad y(0) = 1, \qquad y'(0) = 1 \tag{4.3}$$

Second, solution of $y(x)$ is assumed to be a perturbation expansion:

$$y(x) = \sum_{n=0}^{\infty} \varepsilon^n \, y_n(x) \tag{4.4}$$

where $y_0(0) = 1,\ y_0'(0) = 1,\ and\ y_n(0) = 0,\ y_n'(0) = 0\ \ n \geq 1$

$$\varepsilon^0 y_0"(x) + \varepsilon^1 y_1"(x) + \varepsilon^2 y_2"(x) = \varepsilon[\varepsilon^0 y_0(x) + \varepsilon^1 y_1(x) + \varepsilon^2 y_2(x)]\, f(x)$$

$$\varepsilon^0 y_0"(x) + \varepsilon^1 y_1"(x) + \varepsilon^2 y_2"(x) = [\varepsilon^1 y_0(x) + \varepsilon^2 y_1(x) + \varepsilon^3 y_2(x)]\, f(x)$$

There is no ε^0 term on the right hand side, hencey_0 can be find by using boundary conditions

$$y_0"(x) = 0 \quad \rightarrow \quad y_0(x) = 1 + x$$

And, that approach is applied for other small parameter terms as well:

$$y_1"(x) = \ y_0(x)\, f(x)$$

$$y_2"(x) = \ y_1(x)\, f(x)$$

$$y_n"(x) = \ y_{n-1}(x)\, f(x) \quad y_n(0) = 0, \qquad y_n'(0) = 0 \tag{4.5}$$

In general, any inhomogeneous equation might be solved by the variation of parameter method whenever the solution of the associated homogeneous equation is known. Due to knowing homogeneous part, the solution to Equation (4.5) is

$$y_n = \int_0^x dt \int_0^t y_{n-1}(s) f(s) ds\,, \quad n \geq 1$$

Then, solving each perturbation part and summing them up gives the solution of initial value problem.

$$y(x) = 1 + x + \epsilon \int_0^x dt \int_0^t ds\,(1+s) f(s) + \cdots \tag{4.6}$$

If ε is very small, it can be expected that $y(x)$ will be well approximated by only few terms of the perturbation series. After all, there are three the main steps of perturbation analysis (Bender & Orszag, 1999). Firstly, equation is converted the original into the perturbation problem by introducing the small parameter $\varepsilon \ll 1$. Then, an expression is assumed for the answer in the form of a perturbation series. Finally, answer is recovered to the original by summing the perturbation series.

In this chapter, straight forward expansion method will be used to solve non-linear equation which is defining mathematical model of hot-wire. In this study, work of Beljaars (1976) has been very helpful and guiding to apply perturbation theory into the mathematical model of the hot-wire. The wire supports are much thicker than the wire; so the thermal inertia of supports can be assumed to infinitely large. Thermal inertia is a scalar quantity that provides a measure of material's ability to resist a change in temperature. High thermal inertia materials resist change in temperature while temperatures of low thermal inertia materials respond quickly to changes. Therefore, when supports are assumed to be thick, their temperatures can be considered equal to the ambient air. Secondly, ends of wire will be plated with copper to investigate whether conduction losses falls or not. This time, temperature of plated ends is not considered to be equal to the ambient air.

4.2. Mathematical Modelling of Hot-Wire by Perturbation Method

In the constant-temperature anemometer, the effect of thermal inertia is reduced by using electronic feedback system to control the resistance and hence the average temperature of wire. In ideal case, corresponding time constant of system will be zero, but this is only achieved by keeping local wire temperature truly constant (Beljaars, 1976). Instead of this, electronic circuit adjusts the wire resistance to keep it constant. As mentioned before, temperature distribution is not uniform along the wire as the results of heat conduction to the prongs. Also, local wire temperature depends on the heat transfer coefficient. If the latter is time dependent, as in the case of a turbulent

flow, the temperature profile will be time dependent as well. And this effect introduces certain thermal inertia. Then, thermal inertia affect the dynamics of hot-wire.

Mathematical treatment of wire needs some simplifications. Firstly, wire material properties are independent of temperature. Secondly, ambient temperature is constant during the fluid flow, and also heat transfer coefficient is uniform over the wire length. Heat-rate balance Equation (2.13) can be rewritten as a:

$$\frac{1}{4}\pi \mathrm{D}^2 \rho \, \mathrm{c}_w \, \frac{\partial \mathrm{T}}{\partial t} = \frac{1}{4} \, \pi \, \mathrm{D}^2 \, k \, \frac{\partial^2 T}{\partial x^2} + I^2 R_w - T \, \pi \, D \, h \tag{4.7}$$

where ρ is the density of wire, c is the specific heat of wire and k is the thermal conductivity of wire.

In Equation (4.7), T defines that difference between local temperature of the wire and the ambient temperature, $T' - T_a$.

When the supporting wires are thick the boundary conditions are:

$$T(\pm\frac{1}{2}\mathrm{L}) = 0 \tag{4.8}$$

The anemometer circuit provides the “constant temperature condition”:

$$\frac{1}{L}\int_{-\frac{1}{2}\mathrm{L}}^{\frac{1}{2}\mathrm{L}} T \, dx = \mathrm{T}_{w,m} - \mathrm{T}_a \tag{4.9}$$

The resistance is assumed to be linearly dependent on temperature:

$$\mathrm{R}_w = \mathrm{R}_0 \, (1 + \beta \, T) \tag{4.10}$$

Aim is to calculate the variation of Joule energy due to fluctuations of heat transfer coefficient. Some simplifications are made in notation in order to avoid complexity.

$$\mathrm{p} = \frac{1}{4}\pi \mathrm{D}^2 \rho \, \mathrm{c}_w$$

$$\mathrm{q} = \frac{1}{4} \, \pi \, \mathrm{D}^2 \, k$$

$$f = \pi\, D\, h\ \ (Input\ variable)\ ;\ \ g = I^2 R_0\ \ (Output\ variable)$$

With simplifications of notation, the differential equation becomes

$$p\frac{\partial T}{\partial t} = \mathrm{q}\frac{\partial^2 T}{\partial x^2} + g\ (1 + \beta\ T) - T\ f \tag{4.11}$$

Then, input variable is divided into two parts as stationary part f_0 and time dependent part $\varepsilon\ f_1(t)$. Time depended part can be thought as fluctuation (perturbation) part. It is considered that the time depended part is small when compared with the stationary part.

$$f = f_0 + \varepsilon\ f_1(t) \tag{4.12}$$

Therefore, perturbative solutions for T and g are constructed as a series of power series:

$$T = T_0(x) + \varepsilon\ T_1(x,t) + \varepsilon^2 T_2(x,t) \tag{4.13}$$

$$g = g_0 + \varepsilon\ g_1(t) + \varepsilon^2 g_2(t) \tag{4.14}$$

Substituting Equation (4.13) and (4.14) into (4.11) and equating the same power of ε yields (Beljaars, 1976):

$$\varepsilon^0\text{:} \qquad 0 = \mathrm{q}\frac{\partial^2 T_0}{\partial x^2} - \ T_0(f_0 - \beta\ g_0) + g_0 \tag{4.15}$$

$$\varepsilon^1 :\quad p\frac{\partial T_1}{\partial t} = \mathrm{q}\frac{\partial^2 T_1}{\partial x^2} - \ T_1(f_0 - \beta\ g_0) - T_0(f_1 - \beta\ g_1) + g_1 \tag{4.16}$$

$$\varepsilon^2 :\quad p\frac{\partial T_2}{\partial t} = \mathrm{q}\frac{\partial^2 T_2}{\partial x^2} - \ T_2(f_0 - \beta\ g_0) - T_1(f_1 - \beta\ g_1) + g_2\ (1 + \beta\ T_0) \tag{4.17}$$

The boundary conditions and constant temperature conditions are:

$$T_n\left(\pm\frac{1}{2}\mathrm{L}\right)=0,\quad \mathrm{n}=0,1,2 \tag{4.18}$$

$$\frac{1}{L}\int_{-\frac{1}{2}\mathrm{L}}^{\frac{1}{2}\mathrm{L}} T_0(x)\,dx=\mathrm{T}_w-\mathrm{T}_a\ ;\quad \frac{1}{L}\int_{-\frac{1}{2}\mathrm{L}}^{\frac{1}{2}\mathrm{L}} T_n(x)dx=0\,,\quad \mathrm{n}\geq 1 \tag{4.19}$$

The solution of the stationary temperature distribution is:

$$T_0(x)=2\,\mathrm{A}_1\cosh x\left(\left(\frac{f_0-\beta\,g_0}{q}\right)^{\frac{1}{2}}\right)+\frac{g_0}{f_0-\beta\,g_0} \tag{4.20}$$

The constant A_1 is determined from the boundary condition. The solution of this equation contains implicitly unknown g_0 which is determined from constant temperature condition. This result gives an algebraic equation for g_0. Physical meaning of g_0 is to provide required joule energy per unit length to the wire for stationary condition.

In order to solve Equation (4.16), f_1 is taken to be harmonic in time:

$$f_1=\widehat{f_1}e^{i\omega t} \tag{4.21}$$

Then solution has to be of the form:

$$T_1=\widehat{T_1}e^{i\omega t}\qquad g_1=\widehat{g_1}e^{i\omega t} \tag{4.22}$$

When substitutions are put in Equation (4.16), it becomes:

$$q\frac{\partial^2\widehat{T_1}}{\partial x^2}-\widehat{T_1}(f_0-\beta\,g_0+i\omega p)=T_0\left(\widehat{f_1}-\beta\,\widehat{g_1}\right)-\widehat{g_1} \tag{4.23}$$

Equation (4.23) can be solved by means of Green's Function.

The second order inhomogeneous differential equation with homogeneous boundary conditions can be solved easily with Green's Function. The second order inhomogeneous equation is shown as:

$$L[y] = y'' + p(x)y' + q(x)y = f(x), \qquad for\ a < x < b,$$

where the L is a differential operator and subject to the homogeneous boundary conditions:

$$B_1[y] = B_2[y] = 0$$

We can represent the solution of the inhomogeneous problem as an integral involving the Green's function. It has the solution (Churchill, 1958)

$$y = \int_a^b G(x,y)f(y)dy$$

where the Green's function, $G(x,y)$, satisfies the equation and the boundary conditions

$$LG(x,y) = \delta(x-y), \quad for\ a < x < b, \quad B_1[G(x,y)] = B_2[G(x,y)] = 0$$

According to the explanation about Green's function concept, it might be applied to Equation (4.23). Green's function $G(x,y)$ is the solution of:

$$q\frac{\partial^2 G(x,y)}{\partial x^2} - G(x,y)(f_0 - \beta\ g_0 + i\omega p) = \delta(x-y) \qquad (4.24)$$

The boundary condition of Equation (4.24) is:

$$G(\pm\frac{1}{2}\mathrm{L}, \mathrm{y}) = 0 \qquad (4.25)$$

The right hand sight of Equation (4.24) is delta function. The dirac delta function is used in physics to define a "point source". Green's function characterizes the

response of a system to the presence of a point source. Therefore, if it is known how the system reacts to a point source, then we can determine how it reacts to any distribution of point since we can sum up all the contributions.

Then the solution of Equation (4.23) is given by:

$$\widehat{T_1}(\mathrm{x}) = \int_{-\frac{1}{2}\mathrm{L}}^{\frac{1}{2}\mathrm{L}} (T_0(\widehat{f_1} - \beta\, \widehat{g_1}) - \widehat{g_1})\, G(x, y)\ \mathrm{dy} \tag{4.26}$$

In this equation there is only one unknown quantity which is $\widehat{g_1}$ and it can be found by using constant temperature condition. But integration has to be applied firstly to get algebraic form of $\widehat{g_1}$, then it can be found numerically with making equal integration to constant temperature condition. The complex amplitude of $\widehat{g_1}$ depends on the frequency ω. Physical meaning of $\widehat{g_1}$ is that the reaction of the anemometer power on small harmonic fluctuations of the heat transfer coefficient.

In the Equation (4.17), the term,

$$T_1(f_1 - \beta\, g_1) = \widehat{T_1}(\widehat{f_1} - \beta\, \widehat{g_1})e^{2i\omega t} \tag{4.27}$$

Appears as a source term and thus generates a second harmonic.

Therefore, output variables can be written as:

$$T_2 = \widehat{T_2}e^{2i\omega t} \qquad\qquad g_2 = \widehat{g_2}e^{2i\omega t} \tag{4.28}$$

The equation for $\widehat{T_2}$ becomes:

$$q\frac{\partial^2 \widehat{T_2}}{\partial x^2} - \widehat{T_2}(f_0 - \beta\, g_0 + 2i\omega p) = T_1(\widehat{f_1} - \beta\, \widehat{g_1}) - \widehat{g_2}\,(1 + \beta\, T_0) \tag{4.29}$$

In the same way, Equation (4.29) can be solved by Green's Function which is solution of:

$$q\frac{\partial^2 G_2(x, y)}{\partial x^2} - G_2(x, y)(f_0 - \beta\, g_0 + 2i\omega p) = \delta(x - y) \tag{4.30}$$

with

$$G_2(\pm\frac{1}{2}\mathrm{L}, \mathrm{y}) = 0 \tag{4.31}$$

Then the solution of Equation (4.29) is given by:

$$\widehat{T_2}(\mathrm{x}) = \int_{-\frac{1}{2}\mathrm{L}}^{\frac{1}{2}\mathrm{L}} (\widehat{T_1}(\widehat{f_1} - \beta\, \widehat{g_1}) - \widehat{g_2}\,(1 + \beta\, T_0))\, G_2(x, y)\, \mathrm{dy} \tag{4.32}$$

Similar logic can be applied for $\widehat{T_2}$ as Equation (4.23). After that, $\widehat{g_2}$ is found from the solution by using constant temperature condition.

After performing all cases, it is understood that when the wire is situated in a time dependent velocity field so that

$$f = f_0 + \varepsilon\, \hat{f}_1 e^{i\omega t}$$

the solution for g reads:

$$g = g_0 + \varepsilon\, \widehat{g_1} e^{i\omega t} + \varepsilon^2 \widehat{g_2} e^{2i\omega t}$$

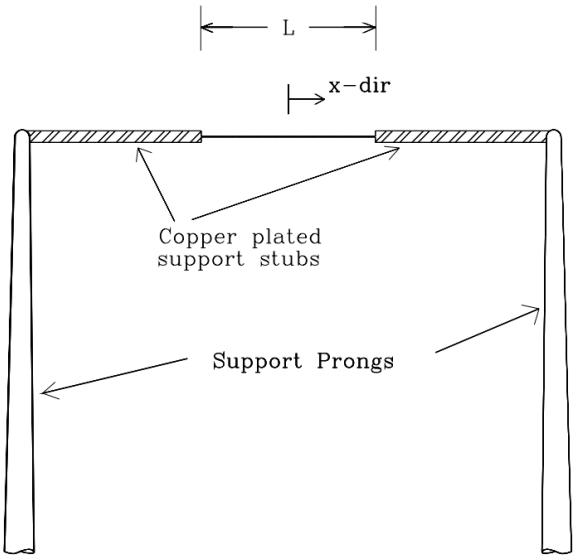

Figure 4.1. Schematic of the simulated plated hot-wire sensor.
(Source: Morris & Foss, 2003)

Until this case, the ends of the wire were assumed to be at ambient temperature. Therefore, the boundary condition $T(\pm\frac{1}{2}\mathrm{L}) = 0$ is only valid for thick supporting wires. This condition changes when ends of the wire plated with copper which can be seen in Figure 4.1. After that, the temperature of wires will be higher than the ambient temperature and will be time dependent. The same differential equation and solution can be applied for copper plated ends as for the measuring wire. Moreover, wire ends are assumed to be too long and the heat production is zero in them. Total length of the wire is L_s.

New expression which is for plated ends becomes ($\frac{L}{2} \leq x \leq \frac{L_s}{2}$)

$$\frac{1}{4}\pi\,\mathrm{D}_{cu}{}^{2}\rho_{cu}c_{cu}\frac{\partial T_{cu}}{\partial t} = \frac{1}{4}\,\pi\,\mathrm{D}_{cu}{}^{2}k_{cu}\frac{\partial^2 T_{cu}}{\partial x^2} - T_{cu}\pi D_{cu}h_{cu} \tag{4.33}$$

In Equation (4.33), $T_{cu}(x,t)$ defines that difference between local temperature of the copper plated support prongs and the ambient temperature, $T'_{cu} - T_a$.

New boundary conditions for plated case become:

$$\begin{gathered}\frac{\partial T}{\partial x} = 0 \quad \text{at} \quad \mathrm{x} = 0 \\ T = T_{cu} \quad \text{at} \quad \mathrm{x} = \frac{1}{2}L \\ \mathrm{D}^2\,\mathrm{k}\,\frac{\partial T}{\partial x} = \mathrm{D}_{cu}{}^{2}\mathrm{k}_{cu}\frac{\partial T_{cu}}{\partial x}\,\text{at} \quad \mathrm{x} = \frac{1}{2}L \\ T_{cu} = 0 \quad \text{at} \quad \mathrm{x} = \frac{La}{2}\end{gathered} \tag{4.34}$$

With simplifications of notation, the differential equation for plated ends becomes:

$$p_{cu}\frac{\partial T_{cu}}{\partial t} = \mathrm{q}_{cu}\frac{\partial^2 T_{cu}}{\partial x^2} - T_{cu}f_{cu} \tag{4.35}$$

where

$$p_{cu} = \frac{1}{4}\pi \, \mathrm{D}_{cu}{}^{2}\rho_{cu}\mathrm{c}_{cu}$$

$$\mathrm{q}_{cu} = \frac{1}{4}\,\pi \, \mathrm{D}_{cu}{}^{2}k_{cu}$$

$$f_{cu} = \pi D_{cu} h_{cu}(Input\ variable)$$

These boundary conditions show following physical requirements:

i. A temperature distribution along the heated wire is symmetrical about the origin of x axis.
ii. The temperature of copper plated end is equal to that of the active wire at the interface.
iii. Heat flowing through the interface is assumed to be conserved.
iv. Temperature at the tip of the prong is equal to fluid temperature.

In this case, perturbation method is applied both of the wire and plated ends. Therefore, perturbative solutions for T_{cu} is constructed as a series of power series:

$$T_{cu} = T_{cu0}(x) + \varepsilon\, T_{cu1}(x,t) + \varepsilon^2 T_{cu2}(x,t) \qquad (4.36)$$

Substituting Equation (4.36) into (4.35) and equating same power terms of ε yields:

$$\varepsilon^0: \qquad 0 = \mathrm{qu}\frac{\partial^2 T_{cu0}}{\partial x^2} - \, T_{cu0} f_{cu0} \qquad (4.37)$$

$$\varepsilon^1: \qquad pu\frac{\partial T_{cu1}}{\partial t} = \mathrm{qu}\frac{\partial^2 T_{cu1}}{\partial x^2} - \, T_{cu1} f_{cu0} - T_{cu0} f_{cu1} \qquad (4.38)$$

$$\varepsilon^2 \qquad : \qquad \mathrm{pu}\,\frac{\partial \mathrm{T_{cu2}}}{\partial \mathrm{t}} = \mathrm{qu}\,\frac{\partial^2 \mathrm{T_{cu2}}}{\partial \mathrm{x}^2} - \, \mathrm{T_{cu2}}\,\mathrm{f_{cu0}} - \mathrm{T_{cu1}}\mathrm{f_{cu1}} \qquad (4.39)$$

The new boundary conditions have to be obtained by applying perturbation method into them. Equating terms with the same power technique should be repeated for coupled boundary conditions.

$$\frac{\partial T_0}{\partial x} + \varepsilon \frac{\partial T_1}{\partial x} + \varepsilon^2 \frac{\partial T_2}{\partial x} = 0 \quad \text{at} \quad x = 0$$

$$\frac{\partial T_0}{\partial x} = 0, \quad \frac{\partial T_1}{\partial x} = 0, \quad \frac{\partial T_2}{\partial x} = 0 \tag{4.40}$$

$$T_0 + \varepsilon\, T_1 + \varepsilon^2 T_2 = T_{cu0} + \varepsilon\, T_{cu1} + \varepsilon^2 T_{cu2} \quad \text{at} \quad x = \frac{1}{2}L \tag{4.41}$$

$$T_0 = T_{cu0}, \quad T_1 = T_{cu1}, \qquad T_2 = T_{cu2}$$

$$\begin{aligned} &D^2\, k\, \frac{\partial T_0}{\partial x} + \varepsilon D^2\, k\, \frac{\partial T_1}{\partial x} + \varepsilon^2 D^2\, k\, \frac{\partial T_2}{\partial x} = D_{cu}{}^2 k_{cu} \frac{\partial T_{cu0}}{\partial x} + \\ &\varepsilon\, D_{cu}{}^2 k_{cu} \frac{\partial T_{cu1}}{\partial x} + \varepsilon^2 D_{cu}{}^2 k_{cu} \frac{\partial T_{cu2}}{\partial x} \quad \text{at} \quad x = \tfrac{1}{2}L \\ &D^2\, k\, \frac{\partial T_0}{\partial x} = D_{cu}{}^2 k_{cu} \frac{\partial T_{cu0}}{\partial x}, \\ &D^2\, k\, \frac{\partial T_1}{\partial x} = D_{cu}{}^2 k_{cu} \frac{\partial T_{cu1}}{\partial x}, \\ &D^2\, k\, \frac{\partial T_2}{\partial x} = D_{cu}{}^2 k_{cu} \frac{\partial T_{cu2}}{\partial x} \end{aligned} \tag{4.42}$$

With using boundary conditions, time dependent copper plated temperature profile can be found simply by computer program. After that, outputs of active wire with new boundary conditions are obtained the by following sequence of previous section.

CHAPTER 5

RESULT AND DISCUSSION

In first part, analytical solution for heat transfer equation of hot-wire is presented. Heated wire is exerted in air flow by forced convection. By this way, it can be understood the general behavior of hot-wire at varying sensor parameters. Temperature distribution along it and conduction end losses are presented with these conditions. Also, effect of radiation term in heat transfer equation is investigated. Then, obtained results are compared with the literature.

In previous chapter, perturbation method has been applied for the time dependent differential equation of a constant temperature anemometer. In second part, this theory is performed in heat-rate balance equation to investigate dynamic response of the wire. Also, the influence of thin supporting wires, or copper-plated wire ends, is studied.

5.1. Static Characteristics of Hot-Wire

In this part, numerical and analytical investigations have been performed for Equation (2.13) by using MATLAB (MathWorks Inc.). Single sensor of the hot-wire probe is used with tungsten wire. Sensor parameters are 1.25 mm in length and 5 μm in diameter. All the physical properties of tungsten are taken at film temperature.

In theory of operation part, energy balance for heated wire has been derived. As mentioned before, heat loss comes from conduction, convection and radiation terms. Indeed, major effect is for the convection term. In theory part, radiation effect was neglected according to the literature. Therefore, radiation effect on heat transfer is presented firstly. This study is investigated at maximum wire temperature. Hence, conduction term can be neglected to evaluate radiation effect. This routine, "ode45" uses a variable step Range-Kutta Method to solve differential equations numerically. Figure 5.1 shows the temperature variations of hot-wire as function of time at different flow velocities. As velocities increases, convective heat transfer becomes more effective on heat transfer. Therefore, wire temperature decreases with increasing velocity. Then,

the same equation was solved again without radiation term and drawn a plot (see Figure 5.2). In order to see effect of radiation, these two studies have been subtracted in each other and plotted again (see Figure 5.3). It shows that radiation term can be neglected because of very small differences, especially at high and moderate velocities. Radiation might be effective at low velocities or very high temperatures. According to the results, neglecting of radiation term seems logical. This conclusion agrees with studies of A. Al-Salaymeh (2005) and Manshadi & Esfeh (2012). Therefore, radiation term has been not put in following results.

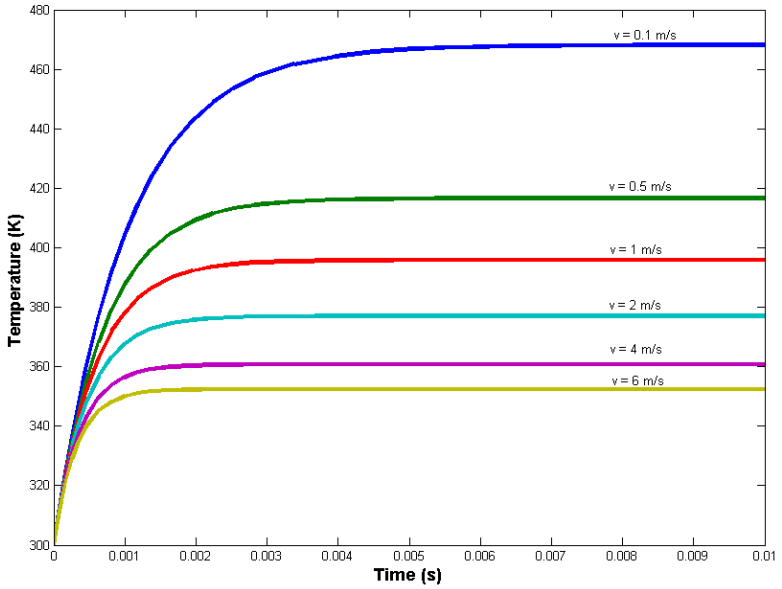

Figure 5.1. Temperature variations of hot-wire as function of time at different flow velocities.

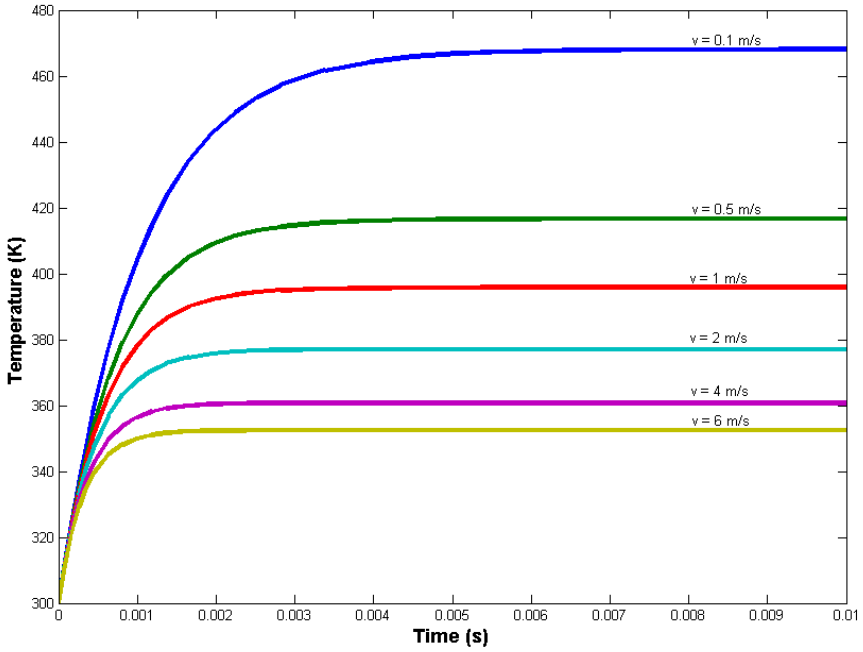

Figure 5.2. Temperature variations of hot-wire without radiation term as function of time at different velocities.

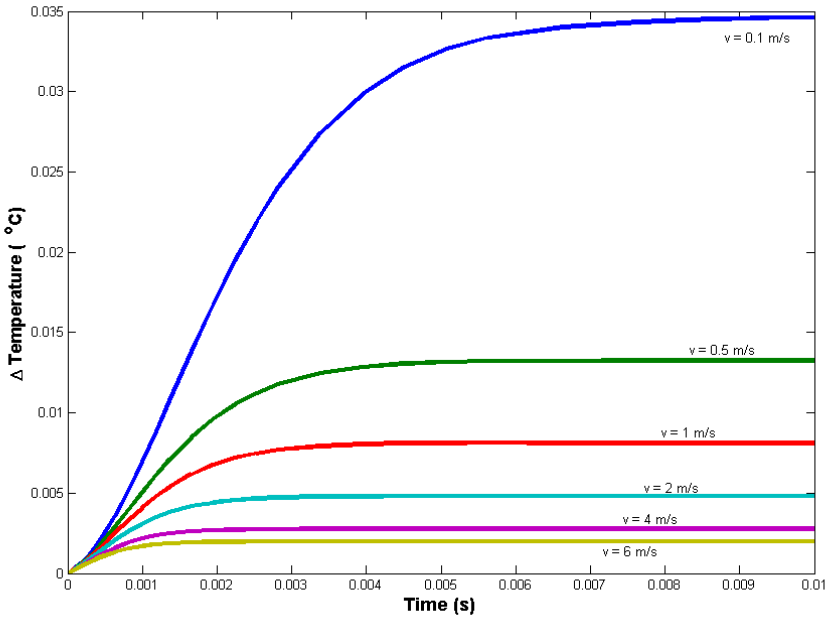

Figure 5.3. Temperature difference variations of hot-wire without radiation term as function of time at different velocities.

Non-dimensional form of steady state temperature distribution along the hot-wire has been obtained as Equation (2.22). The temperature distributions for varying

lengths are drawn in Figure 5.4. Diameter of wire is 5 μm and air velocity is taken as 10 m/s. Convective heat transfer term plays more important role on hot-wire operation by increasing length of wire. It can be easily understood that the temperature distribution along the wire becomes more uniform if longer length wire is used. By this means, temperature at different part of the wire approaches easily to mean temperature. Temperature fluctuations would be minimized along the wire. Therefore, it provides to reduce thermal transient effects. Also, Figure 5.4 shows that behavior coincides with the previous works which have been carried by Davies & Fisher (1964), A. Al-Salaymeh (2005) and Manshadi & Esfeh (2012).

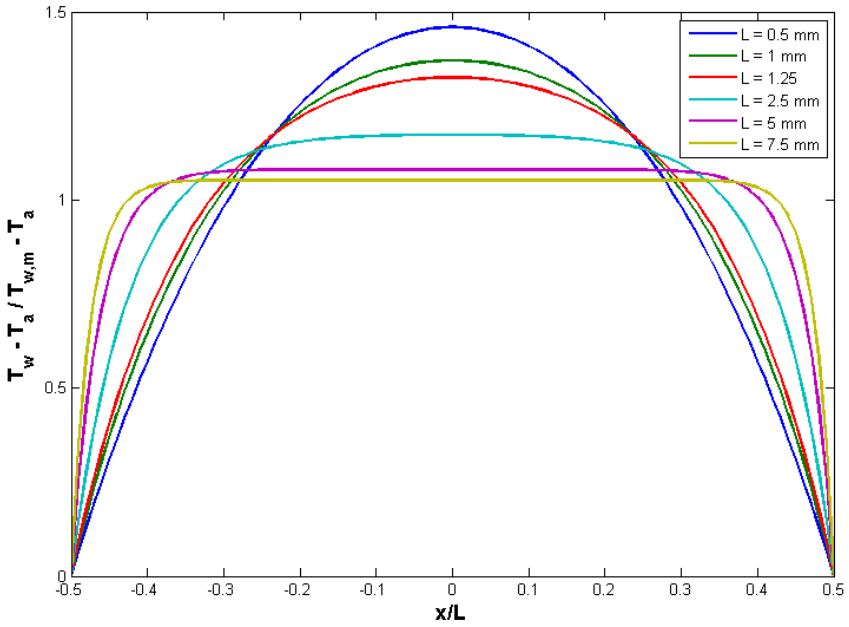

Figure 5.4. Temperature distribution along the hot-wire for different length.

Conductive end losses are reduced with increasing length of wire. As it is shown in Figure 5.5, ratio of conduction (means conduction end losses) to the overall heat transfer decreases for longer wires. However, reduction rate diminish as wire length increases. The reason of that can be explained by mathematically. The maximum value of $\tanh(|K_1|^{1/2}\, l/2)$ is about 1, therefore approaching the wire length to its critical value will not cause a significant reduction. This finding suggest in favor of longer wires. However, as will be mentioned next section, there are other persuasive reasons for using shorter wires.

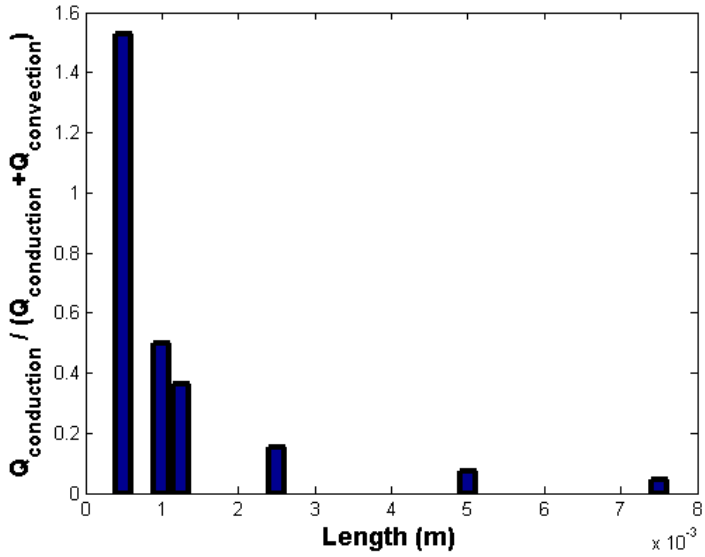

Figure 5.5. Conduction-total heat transfer ratio for different length.

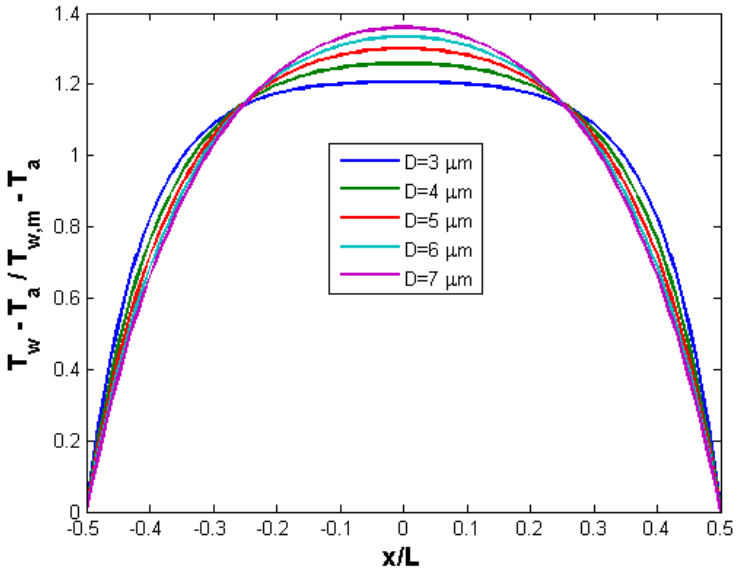

Figure 5.6. Temperature distribution along the wire for different diameter.

Figure 5.6 shows the varying non-dimensional temperature distribution with respect to diameter. Length of wire is 1.25 mm and air velocity is taken 10 m/s. As diameter increases, cross section area increases, too. As it can be seen in Equation (2.24), conduction to the prongs directly rises with increasing area. As mentioned before, conduction to the prongs causes to break down the uniformity of temperature distribution along the heated wire. Therefore, plot becomes pointed with increasing diameter.

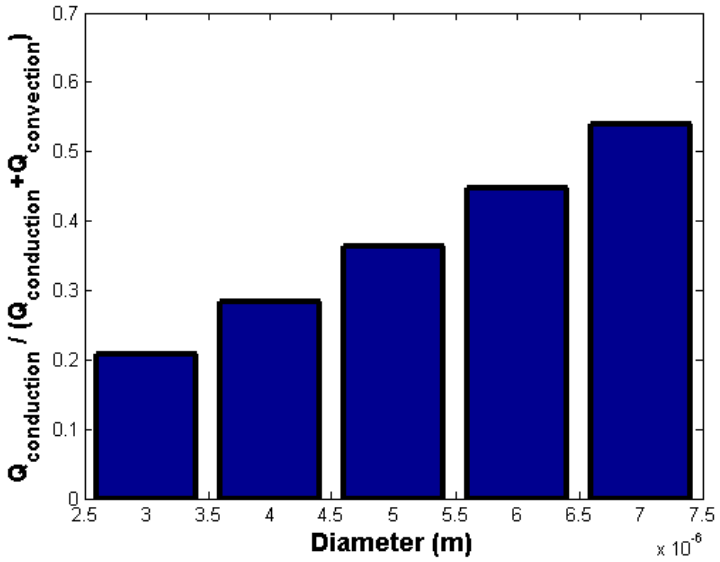

Figure 5.7. Conduction-total heat transfer ratio for different diameter.

Figure 5.7 proves that conduction-convection heat transfer ratio rises up due to higher conduction term when diameter increases. It can be concluded that it is useful to choose the lower diameter, but it should be noted that strength of wire material decreases in this way. Probe brakeage is the worst side of the hot-wire anemometry. Hinze (1975) has already specified 2.5 μm in diameter which is required for minimum strength. All these taken into consideration, diameter range of heated wire can be taken as 2.5 μm to 5 μm for fluid flow operations.

5.2. Dynamic Characteristics of Hot-Wire

5.2.1. **Single Wire Analysis**

Basic operation of hot-wire anemometer is based upon a perfect equilibrium between the heat developed by the electronic current and the heat transferred to the following fluid. If the fluctuations of fluid flow changes quickly, the wire must be heated and cooled with the same frequency. This can be only possible if the thermal inertia of wire is infinitely small. However, thermal inertia has finite value and due to this reason, there is a delay between the fluctuations of the fluid velocity and the corresponding fluctuations of the heated wire. Because of this reason, thermal inertia affects the dynamic characteristic of the wire. For accurate turbulent measurements, it is

significant to have uniform amplitude response of the wire over the working frequency range.

Outputs of hot-wire have been derived in previous chapter. Air is the cold surrounding fluid. It is assumed that the heat transfer coefficient is changing harmonically as an input. All these statements (system code) were put in order by Mathematica 9 (Wolfram Inc.). Numerical values of for g_0, g_1 and g_2 have been calculated for different practical sensor parameters. Then, algebraic equations for g_0, g_1 and g_2 were solved and drawn by Mathematica 9. Material was chosen as tungsten and the calculations were performed for different situations at 220°C above ambient temperature. Therefore, average wire temperature was attempted to keep constant at 250°C. At the beginning, air velocity was taken as 5 m/s for all situations, but then it varied to see its influence on thermal behavior of heated wire. The stationary heat transfer coefficient was obtained from the Equation (2.30) as the Nu-Re relation of Collis and Williams (1959). The quantity $\widehat{f_1}$ had been taken equal to 1 which did not introduce any restriction by Beljaars (1976). It means that the amplitude of the input variable then equals ε. In this study, it is taken equal to 1.

Firstly, we have assumed that the supports have an infinitely great heat capacity and that their temperature is equal to the ambient temperature. Hinze (1975) said that it was obvious that these assumptions are realistic only if the dimensions of the supports are very large compared with the wire diameter.

In order to show first boundary condition and stationary temperature profile, $T_0(x)$, Figure 5.8 has been drawn. As seen in this plot, temperature of the ends of the wire is equal to ambient, hence $T\left(\pm\frac{L}{2}\right) = 0$.

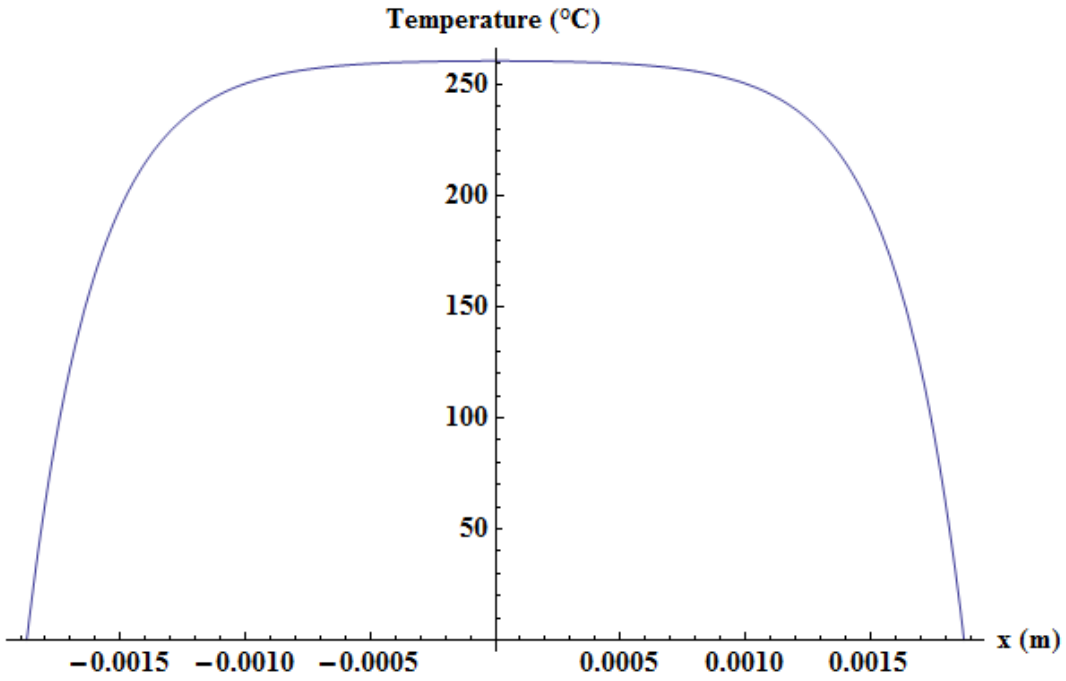

Figure 5.8. Stationary temperature profile of single heated wire, D=5 µm, L=3.75 mm.

Figure 5.9 and Figure 5.10 show the varying amplitude characteristic $|\widehat{g_1}|$ for different length of wires in diameter 3 µm and 5 µm with respect to the circular frequency ω, because input is given harmonic in time. In this study, the amplitude $|\widehat{g_1}|$ is called as the sensitivity of wire.

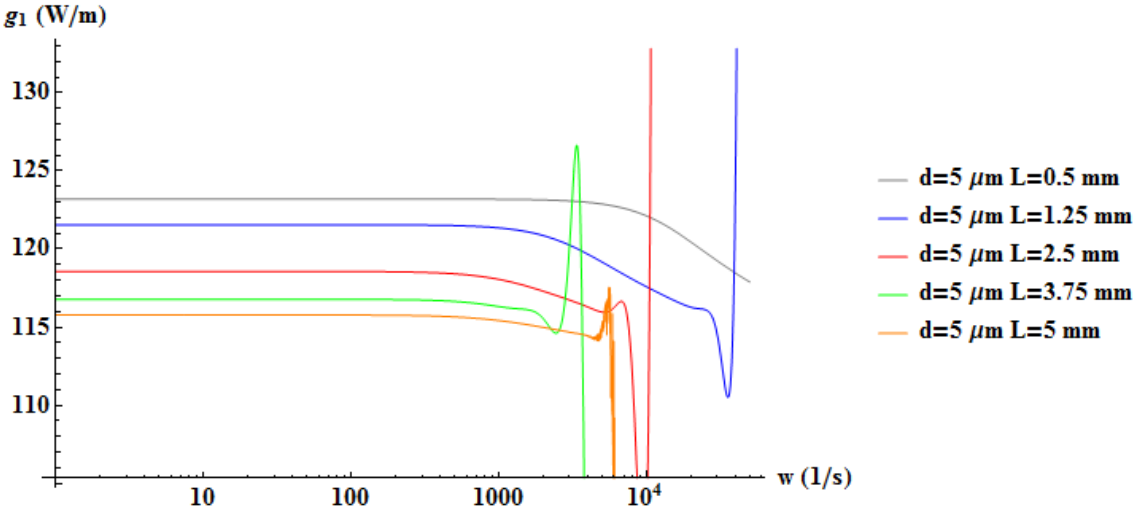

Figure 5.9. Frequency characteristic of hot-wire for various values of length in 5 µm diameter.

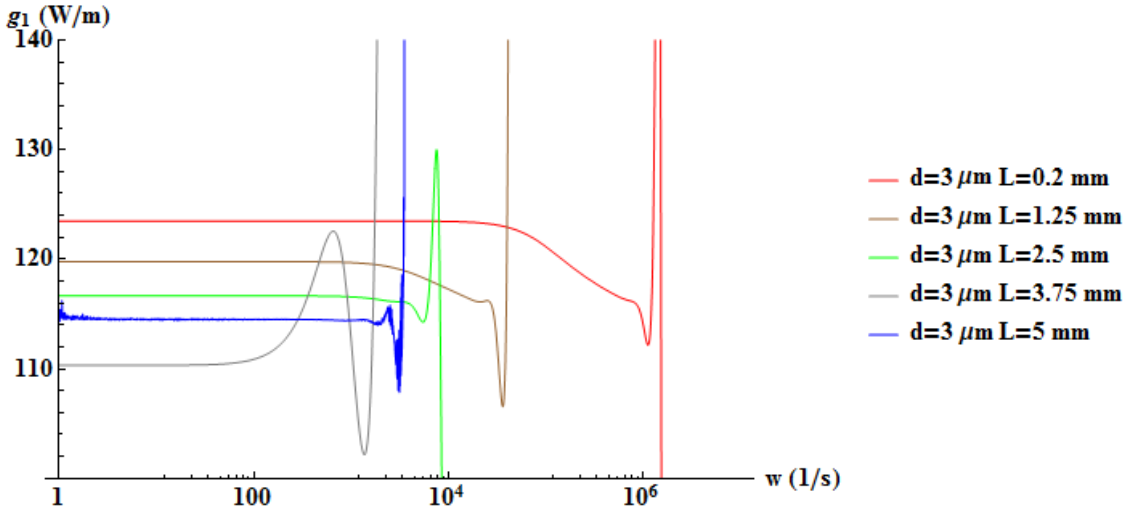

Figure 5.10. Frequency characteristic of hot-wire for various values of length in 3 µm diameter.

Both of them show that sensitivity increases with decreasing length of the wire. When lengths are kept constant but diameter is changing, sensitivity rises up with increasing diameter (see Figure 5.11). For instance, amplitude of gray is almost 122 W/m, but amplitude of blue line is about 120 W/m in Figure 5.11. It seems logical because large diameter needs more energy due to its large heat capacity. In this part, wires which have larger diameter and shorter length can be seen as favorable for operation.

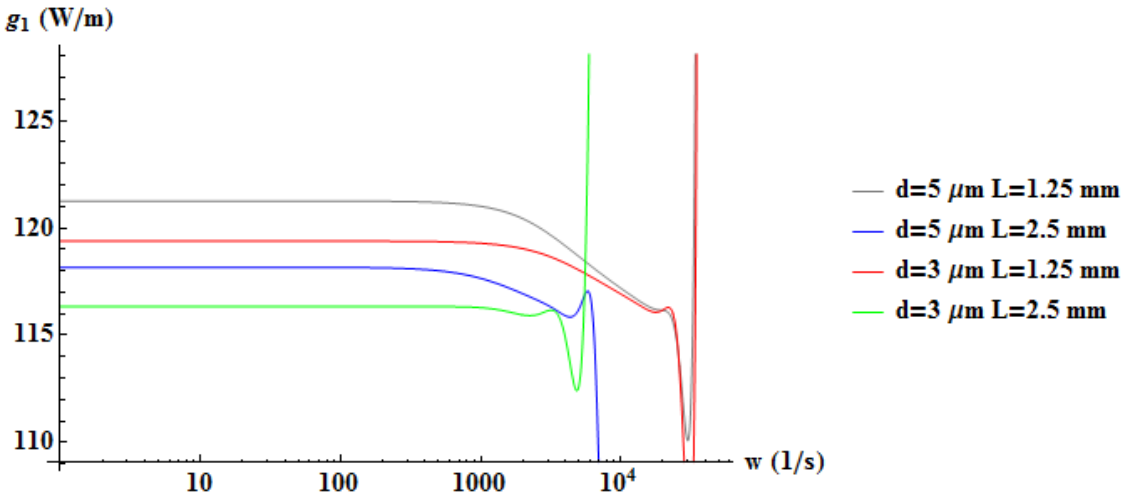

Figure 5.11. Frequency characteristic of hot-wire for various values of length and diameter.

As it can be seen in Figure 5.11, sensitivity values are so close in each other which are changing between 116 W/m and 122 W/m. Therefore, it is more crucial that the amplitude response of anemometer is constant over the frequency range of interest for accurate turbulent measurements. So, key point is the deviation of the flat characteristic of $|\widehat{g_1}|$. To see that clearly, Figure 5.12 was plotted. Dashed lines are the 99% of their sensitivity values and intersection point between sensitivity line and its corresponding dashed line gives the deviation point from the flat line. For example, Sensor A (red line) deviates at 5000 1/s, while in Sensor B (blue line), it deviates at 2700 1/s. Therefore, small diameter should be chosen to get constant amplitude response. Beljaars (1976) introduced the characteristic frequency, which is order of $1/\tau$, where $\tau = \rho\, c\, D/4\, h$ is the time constant. Also, Figure 5.9 and Figure 5.10 show that deviation of the flat characteristic of $|\widehat{g_1}|$ depends on the length of wire. Deviation from the flat characteristics shifts to higher frequencies as the wire length shortens. At the end, the shorter and wire with small diameter can keep its flatness in a broader frequency range which is a desirable property of a wire. Table 5.1 shows that deviation frequencies in presented plots is in the same order with the Beljaars (1976) expression, $1/\tau$.

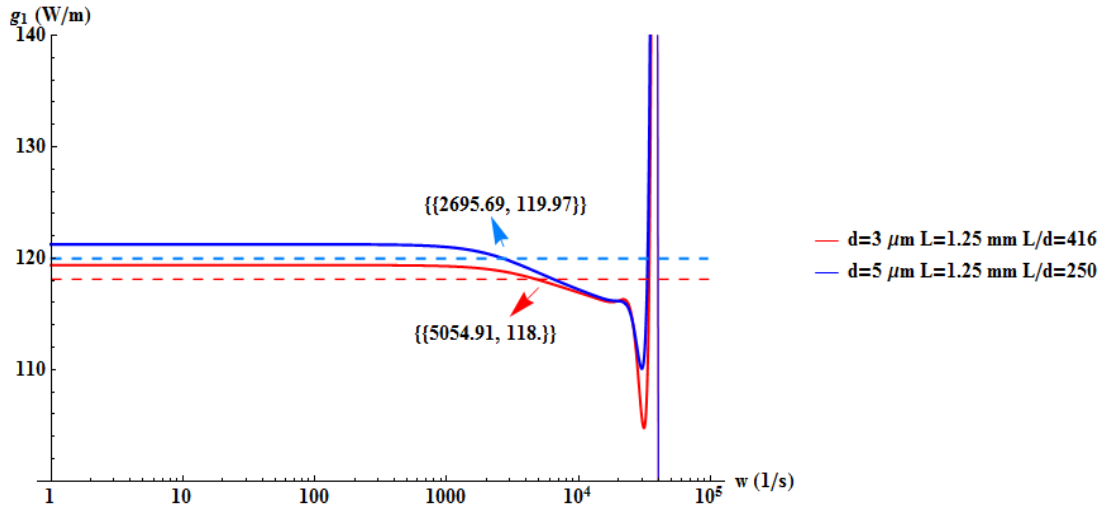

Figure 5.12. Comparison of deviation point for L=1.25 mm case with 3 µm and 5 µm cases.

Table 5.1. Critical frequencies for different sensors.

Sensor Parameters	Beljaars, $1/\tau$ [1/s]	Deviation frequency [1/s]
(A) D=3 µm, L=1.25 mm	≅ 4000	≅ 5000
(B) D=5 µm, L=1.25 mm	≅ 1800	≅ 2700
(C) D=7 µm, L=3 mm	≅ 900	≅ 1000

It should be noted that the work of Beljaars (1976) clearly indicates the plots above.

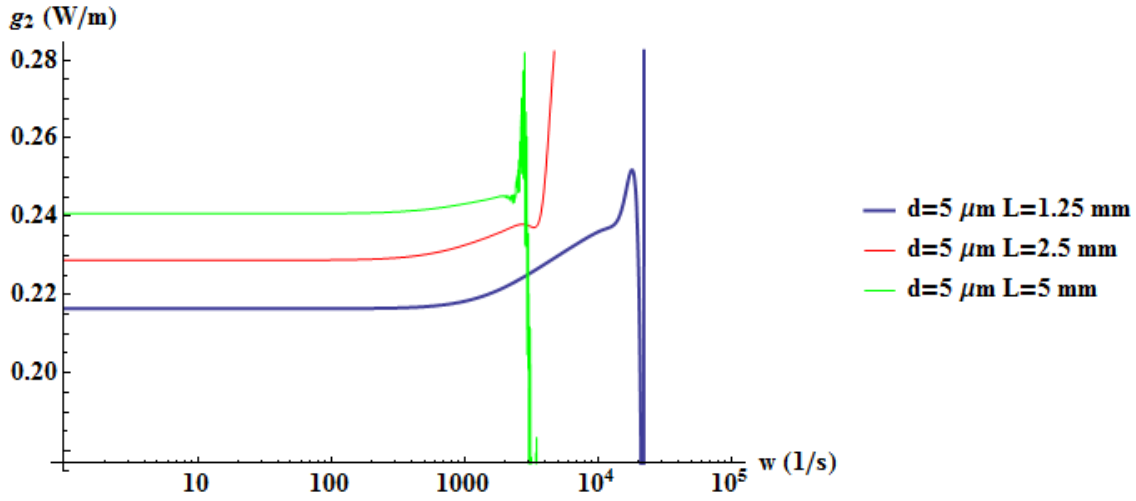

Figure 5.13. Frequency characteristic of the second order correction for various lengths in 5 µm diameter.

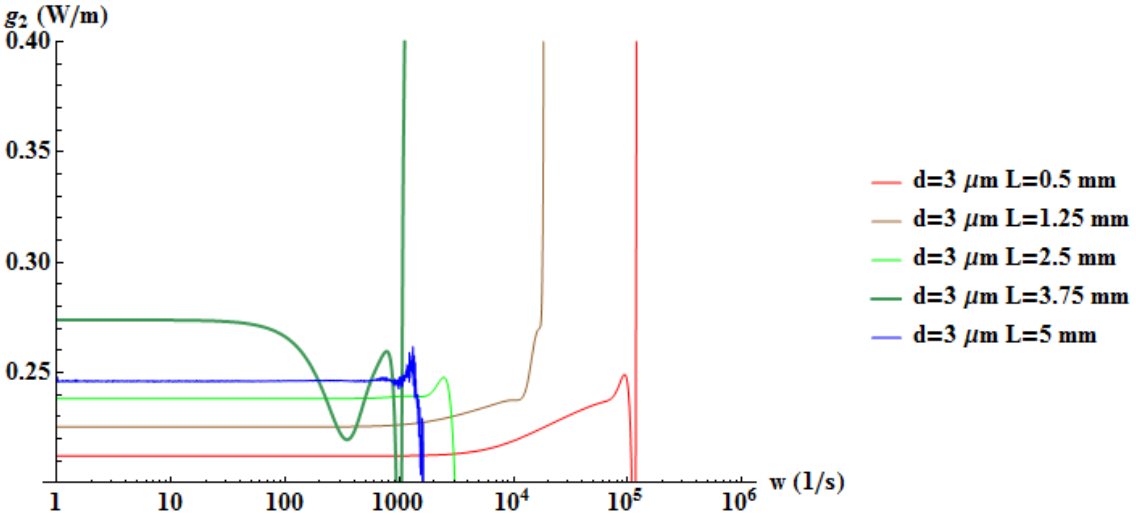

Figure 5.14. Frequency characteristic of the second order correction for various lengths in 3 µm diameter.

Figure 5.13 and Figure 5.14 give the amplitude $|\widehat{g_2}|$ of the second order correction. Aim of plotting second order amplitude $|\widehat{g_2}|$ is to see at what level of turbulent fluctuations the influence of the second order will become of any importance. Second order correction has too low value when compared to $|\widehat{g_1}|$ (see Figure 5.15). Also, this value gets lower while it is multiplying with square of small parameter, ε^2.

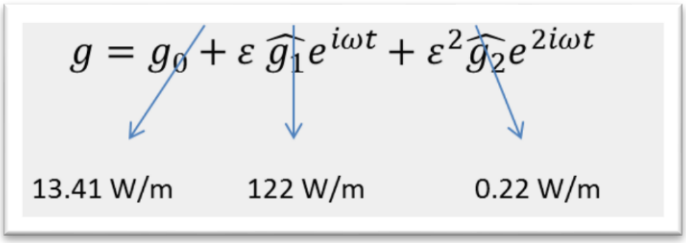

Figure 5.15. Numerical values of g_0, g_1 and g_2 for L=1.25mm in 5 µm diameter.

It can be concluded that a first order expansion is enough even for high turbulent intensities.

According to previous significant investigations, aspect ratio is one of the considerable parameters which need to be examined. Aspect ratio is the length to diameter ratio of the heated wire. Figure 5.16 shows the frequency characteristic with various aspect ratios. High sensitivity values extend between aspect ratio values of 200 and 430. On the other hand, aim is to achieve a uniform frequency response over the range of interest in turbulent measurements. The wires deviate from the flat line at higher frequencies in this region. Also, the wires whose aspect ratios are close to each other have almost the same sensitivity. On the other hand, low sensitivity values are observed at very high aspect ratios such as 750 and 1250. Also, $|\widehat{g_1}|$ deviates from flat characteristic at lower frequencies for high aspect ratios when compared to the others. In addition, very low aspect ratio, 100, exhibits low sensitivity values and deviates earlier. In this regard, Hinze (1975) says that, for platinum-iridium and tungsten wires, the aspect ratio should be higher than 200 to make wire resistance (temperature) almost uniform along the central 60 percent of its length. Moreover, Soe Minn Khine *et al.* (2013) have mentioned that if the aspect ratio becomes smaller than 200, the cooling effect of the wire supports will emerge, and can get worse the frequency response of the hot-wire. It can be concluded that is useful to choose aspect ratio large enough in order to avoid of thermal inertia of the measuring wire and the supporting wires. Besides, looking at the Figure 5.11, some fluctuations have begun to occur at blue line (3 µm in

diameter, 5 mm in length). Its aspect ratio is 1666. Therefore, the present mathematical model of hot-wire is not useful at very high aspect ratios due to unstable behavior.

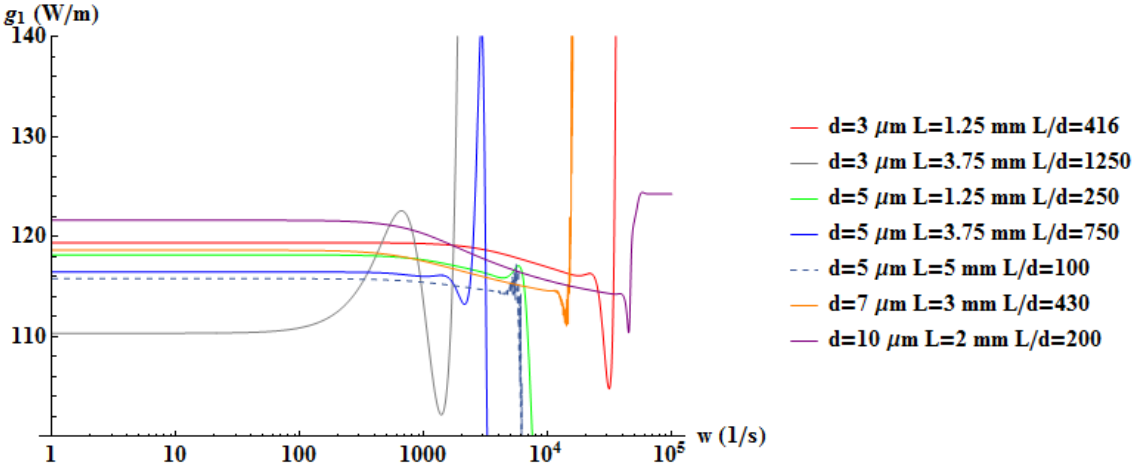

Figure 5.16. Frequency characteristic of hot-wire for various aspect ratios.

5.2.2. **The Wire with Copper-Plated End Analysis**

Up to now, results of frequency characteristic have been given for boundary condition $T(\pm\frac{L}{2}) = 0$. Next, wire with copper-plated ends is investigated for various conditions. As explained in mathematical model of hot-wire, the temperature of wires will be higher than the ambient temperature and will be time dependent. Present results will include sensitivity and frequency characteristic analysis for active wire with plated ends. Heat conducted to the prongs will be studied to understand effects of it on hot-wire operation. For steady state applications conduction losses will be included in the static calibration process. Nevertheless, effect of the conduction losses on the dynamic response of the wire is difficult to examine experimentally, therefore; it needs to be examined theoretically.

In order to show first boundary condition and temperature profile of ends, stationary temperature profile of heated wire has been drawn for a diameter D_{cu} of the copper plated ends of 30 µm. As seen in Figure 5.17, the temperature of the end of the active wire is higher than the ambient temperature. Also, temperature approaches to zero between junction area and end of the plated area (prong) in Figure 5.18. For example, temperature is 13 °C at x=1.85 mm and approaches to zero at x=5 mm. This

shows that the presented mathematical model of heated wire works well with its boundary conditions.

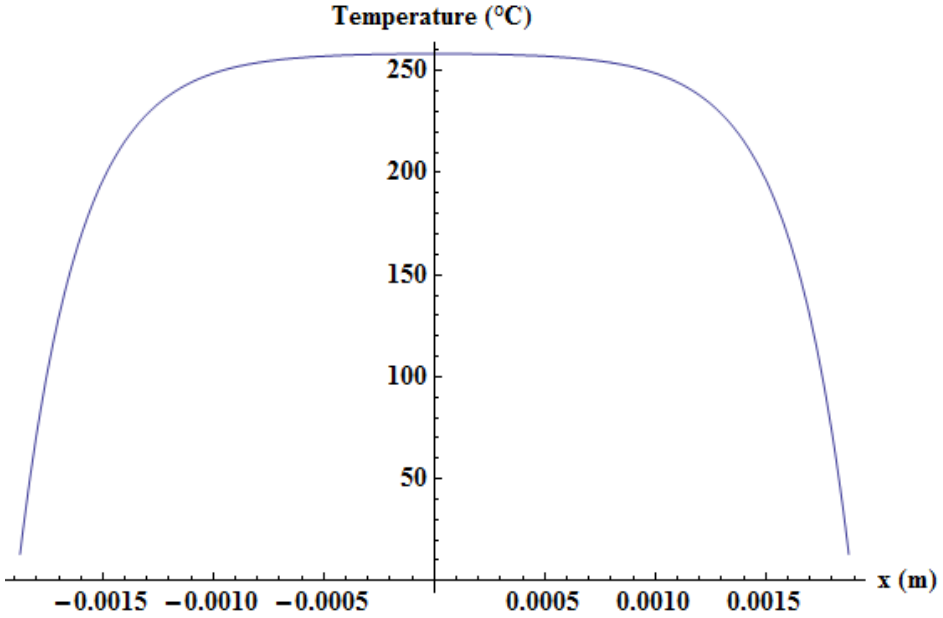

Figure 5.17. Stationary temperature profile of the active wire, D=5 µm L=3.75 mm.

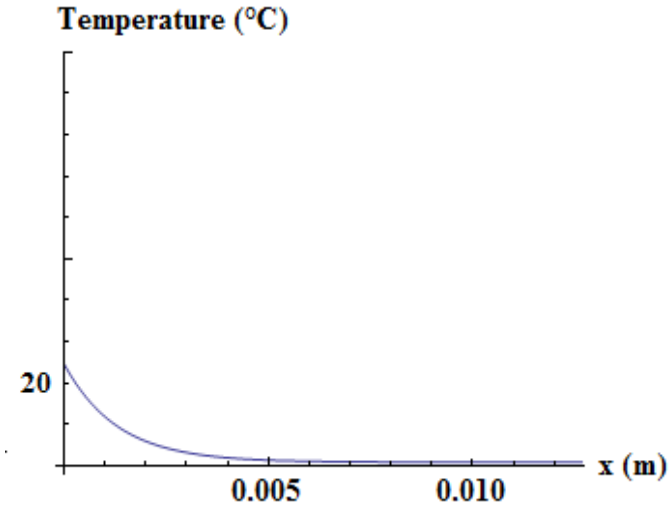

Figure 5.18. Stationary temperature profile of plated end (only right side), D=5 µm L=3.75 mm.

Sensitivity of hot-wire with copper-plated ends is shown in Figure 5.19 and Figure 5.20. At first sight, some plots have two types of characteristic. Actually, this behavior appears in short wires. The first step deviates from the flat line at characteristic frequency and the second corresponding to that of Figure 5.9 and Figure 5.10. On the other hand, long wires exhibits same behavior as for amplitude characteristic in

boundary condition $T(\pm\frac{L}{2}) = 0$. Also, sensitivity behavior looks like the unplated one. It increases with length of the wire.

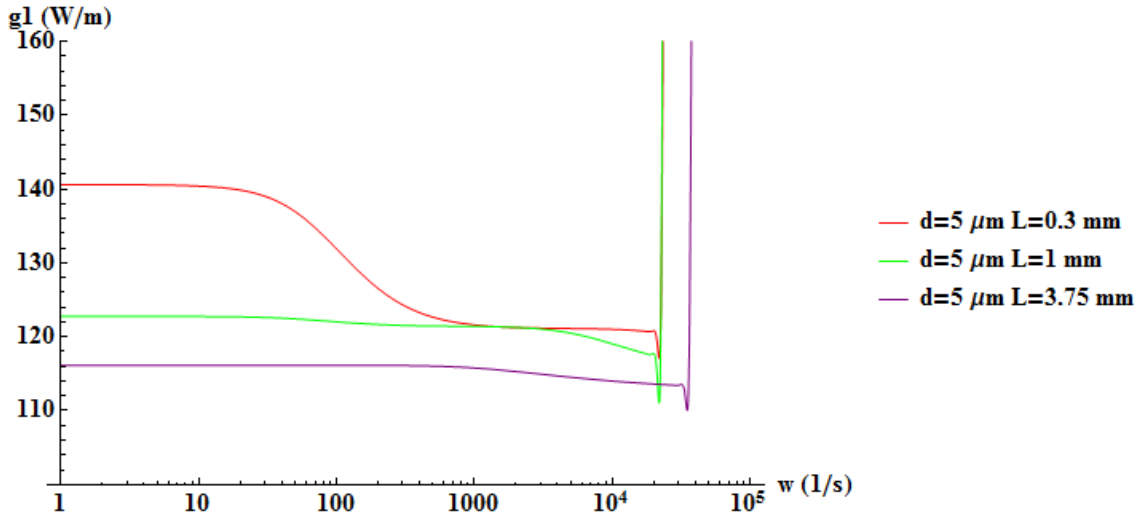

Figure 5.19. Frequency characteristic of hot-wire with copper-plated ends for various values of length in 5 µm diameter.

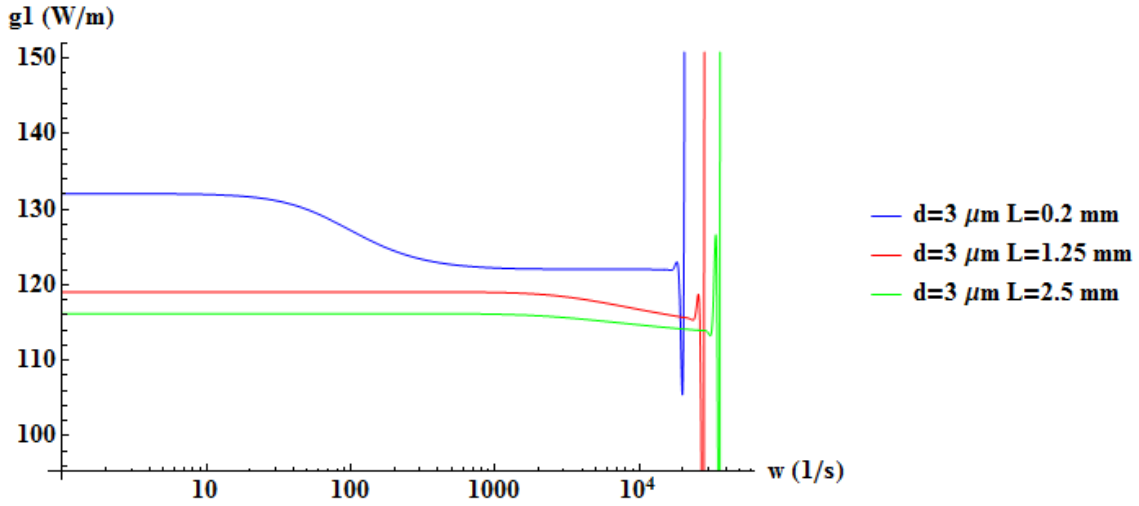

Figure 5.20. Frequency characteristic of hot-wire with copper-plated ends for various values of length in 3 µm diameter.

In copper-plated ends of short wire (less than 1 mm), sensitivity lies on higher level up to characteristic frequency, which is order of $1/\tau_{cu}$, where $\tau_{cu} = \frac{\rho\, c\, \pi\, D_{cu}{}^2}{4\, \pi\, D_{cu}\, h}$ is given by Beljaars (1976). This critical frequency is 72 1/s for copper-plated wire in Figure 5.21, which is order of τ_{cu} ≈230. Then, it turns back the initial level. In order to see this clearly, sensitivities of the shorter wires with copper-plated and unplated ends

are superposed in Figure 5.21 and Figure 5.22. This property favors the use of short wires with copper-plated ends.

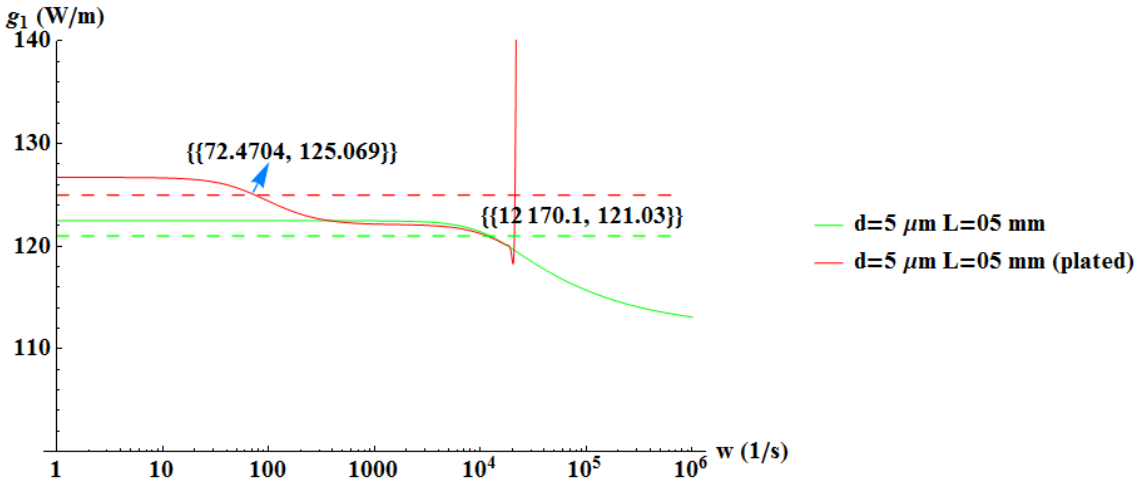

Figure 5.21. Frequency characteristic comparison of single wire and wire with copper-plated ends in 5 µm diameter.

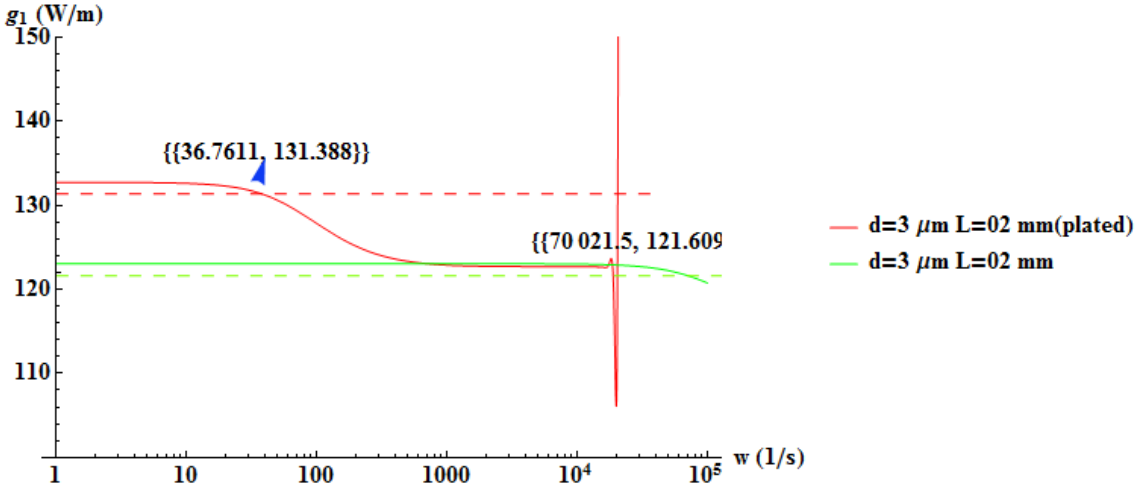

Figure 5.22. Frequency characteristic comparison of single wire and wire with copper-plated ends in 3 µm diameter.

Another question of interest is the effect of various air flow velocity on sensitivity of hot-wire. Bremhorst and Gilmore (1976) expressed that if the perturbation level is low enough and if during the perturbation cycle the wire is at all times in thermal equilibrium with its end supports, ignoring the other mechanical and electrical effects, Equation (5.1) should apply for sensitivity:

$$\frac{\partial \mathrm{E}}{\partial U} = \lim_{\substack{u\to 0 \\ f\to 0}} \frac{e}{u} = \lim_{\substack{u\to 0 \\ f\to 0}} \frac{\overline{e^2}^{1/2}}{\overline{u^2}^{1/2}} \tag{5.1}$$

where E is anemometer output, U is mean flow velocity, f is the perturbation frequency and a bar donates time averaging. Figure 5.23 shows the plots of theoretical and experimental results of sensitivity. It decreases with increasing velocity.

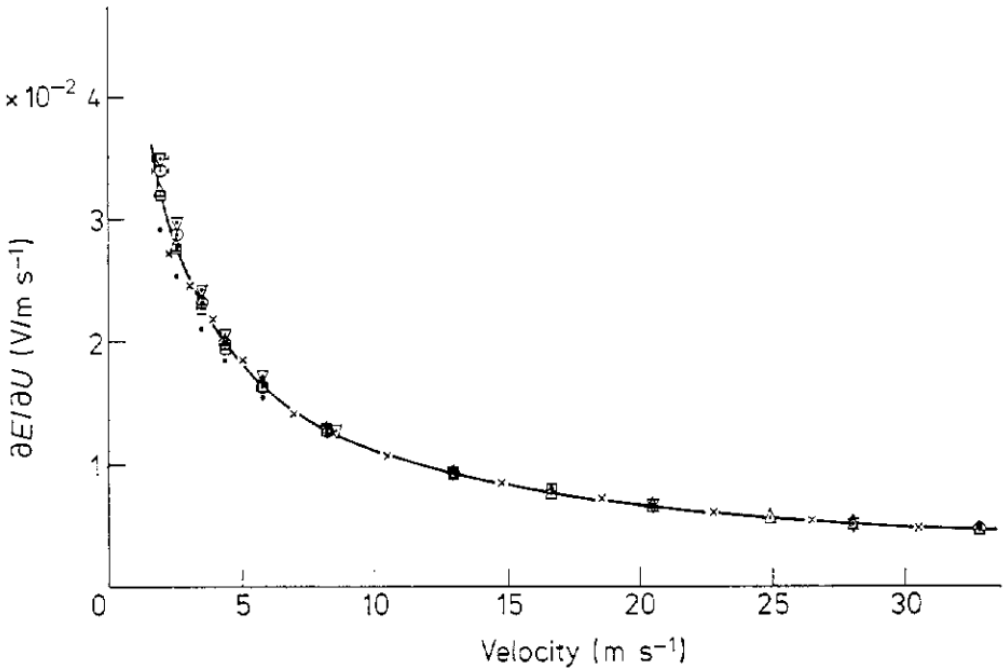

Figure 5.23. Measured calibration coefficients using tungsten wire. -Δ- Siddal and Davies (1972), using both plated and unplated wires; -□- Brunn (1971); -x- Kinns (1973); -•- King's Law. Source: (Bruun, 1996)

Theoretical and experimental results show that the velocity sensitivity decreases at higher velocities. To see effect of velocity variations, a number of conditions have been studied. Sensitivity value becomes too low at higher frequencies (see Figure 5.23). Because of this reason, moderate velocities have been favored for this interest such as 5 m/s, 10 m/s and 15 m/s. Copper-plated wire has been used with 5 μm in diameter and with different length. Figure 5.24 and Figure 5.25 show that sensitivity decreases with increasing velocity. This reduction is more pronounced for short wires. However, at very low velocities, conduction to the prongs may cause overheating through ends of the wire. HWA operation at very low velocities should be done very carefully due to this cooling effect.

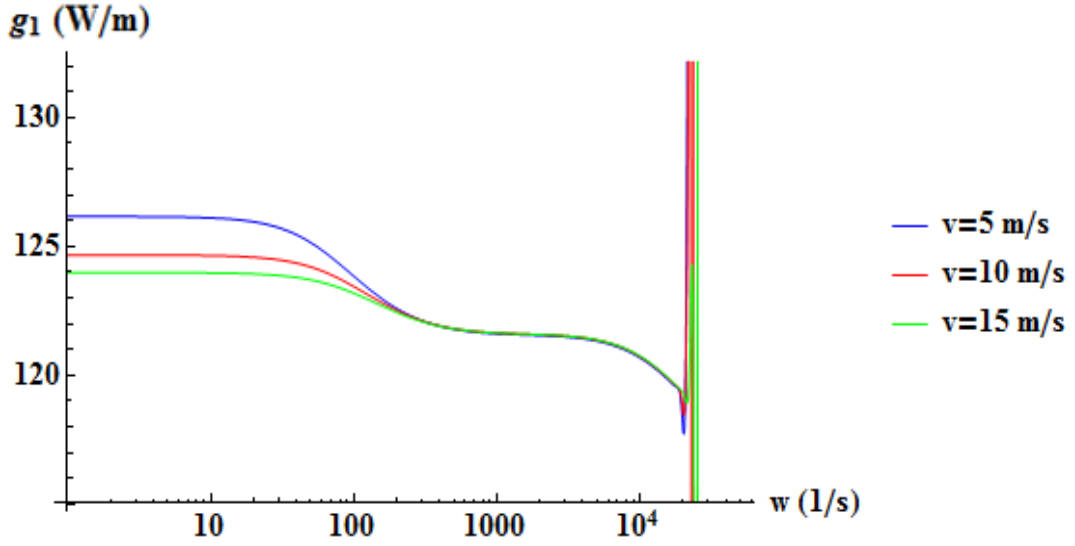

Figure 5.24. Frequency characteristic comparison of the wire with copper-plated ends for different velocities, D=5 μm, L=0.5 mm.

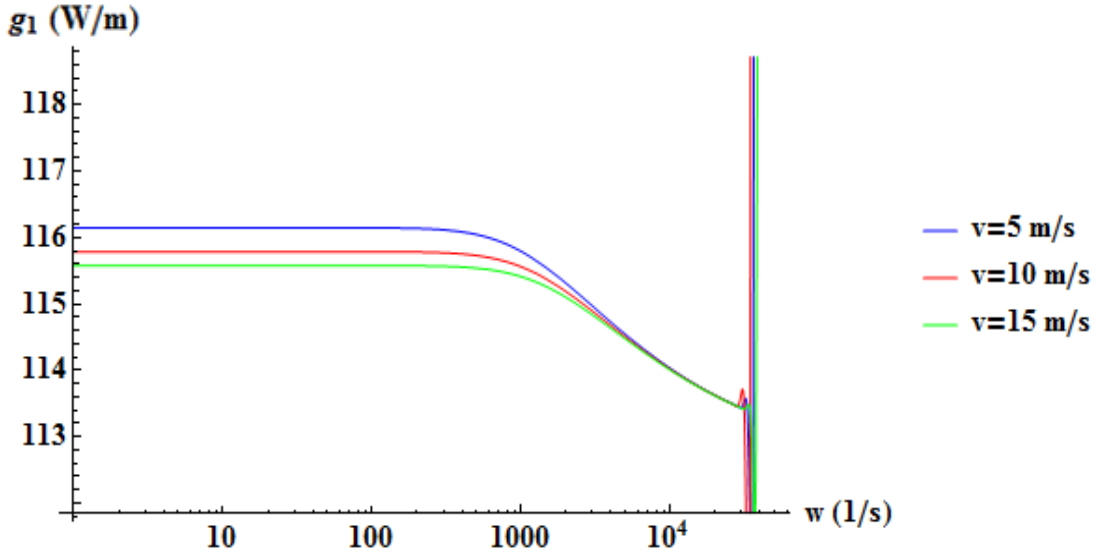

Figure 5.25. Frequency characteristic comparison of the wire with copper-plated ends for different velocities, D=5 μm, L=3.75 mm.

Table 5.2. Heat transfer calculations of the wire with copper-plated ends for various condition.

Length [mm]/Aspect ratio [-]	Velocity [m/s]	Conduction to the prongs (W)	Convection/(Conduction+Convection)
0,1/20	5	0,04293	0,03680
	10	0,04721	0,04404
	15	0,04858	0,04980
0,3/60	5	0,02116	0,19721
	10	0,02172	0,23034
	15	0,02207	0,25347
0,5/100	5	0,01431	0,37702
	10	0,01471	0,42496
	15	0,01497	0,45540
1,0/200	5	0,01073	0,54778
	10	0,01112	0,59453
	15	0,01139	0,62237
1,25/250	5	0,00806	0,72868
	10	0,00853	0,76115
	15	0,00885	0,77995
2,0/400	5	0,00686	0,83458
	10	0,00739	0,85474
	15	0,00781	0,86508
3,75/750	5	0,00618	0,91316
	10	0,00672	0,92378
	15	0,00710	0,92964

According to Table 5.2, conduction term decreases as with increasing velocity for the same aspect ratio. A physical explanation as to why conduction to prongs increases with velocity can be clarified by Morris (2002). Their study suggests that in the conjunction with increasing convective cooling over the hot-wire, temperature distribution along the sensor become as lower temperatures in the middle region of the wire and higher temperatures near the end of the wire (see Figure 5.26). Therefore, temperature distribution exhibits flatter structure at higher velocities. Also, it can be seen clearly seen in Figure 5.1. This behavior leads to increasing temperature gradient at x=L/2 and according to Equation (2.24), conduction to the prongs rises by this way.

This can be thought as an error in the system, but overall heat transfer should be examined for sensible deduction.

Li (2004) indicates that the heat conduction from the heated wire to its prongs is reduced by increasing length to diameter ratio. Present theoretical results Table 5.2 agree with results of Li (2004). When aspect ratio rises, the heat losses from the end of the wire by conduction become relatively less than from convection.

Goldstein (1996) notes that for research work, 2.5 to 5 μm are the most common, with the aspect ratios, L/d of 100 to 600 and commercially mounted wires typically have $L/d \cong 300$. Present theoretical results give an aspect ratio range from 200 to 430 for better sensitivity value and frequency range. Therefore, current investigation is fit into the given range and aspect ratio of commercially mounted wires is in the present range found by perturbation theory.

As mentioned in previous section 5.1 and Table 5.2, temperature distribution along the heated wire becomes flatter and conduction to the prongs is reduced with using long wires. This would seem to favor long wires for HWA operations. However, there are other important reasons to favor the shorter wires. As it is known, velocity distributions in turbulent flow are not uniform and they vary down to micro scale of turbulence. Hinze (1975) mentions that for making true point measurements, the active length of the heated wire should not exceed 0.5 mm, even for turbulent flows of moderate average velocity. In addition, sensitivity analysis favors the use of short wires. Also, for aerodynamic efficiency of HWA, the wires should be as short possible. On the other hand, wire cannot be too short both due to cooling effect of the supports and blocking effect of the prongs. Cooling effect is exerted on the wire by conduction to the supports owing to temperature difference between wire and supports. If wire is too short, the heat by conducted to the supports may reach at dangerous level. Moreover, it would be difficult to build up the sensor if the wire shorter is shorter than 0.5 mm. Active wire can be taken as short as possible with plating ends of it. By this way, probes would be constructed easier.

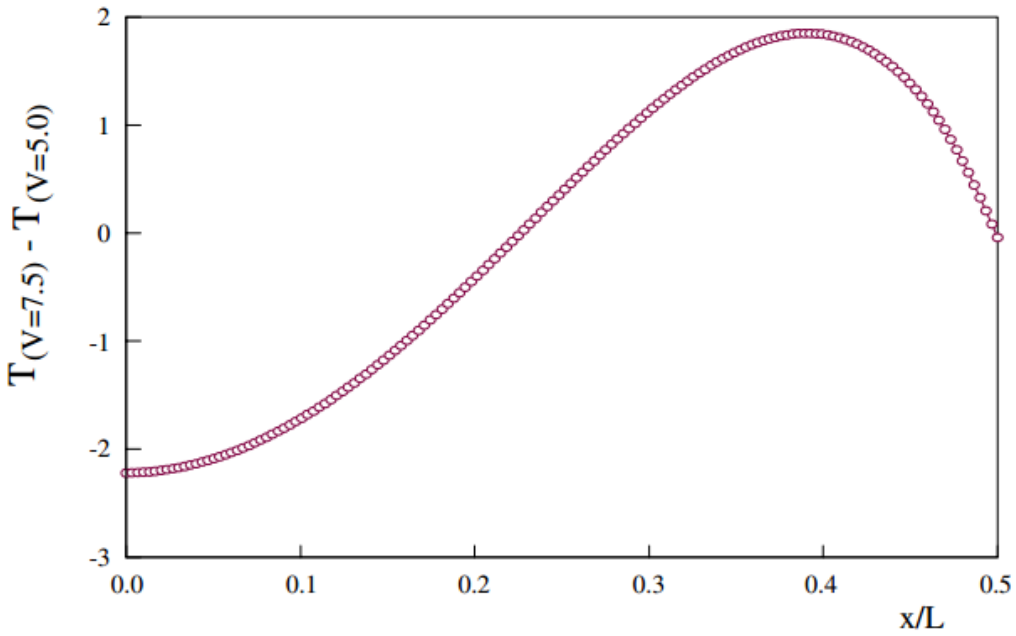

Figure 5.26. Steady state temperature difference from V=5.0 to V=7.5 m/s.
(Source: Morris & Foss, 2003)

Table 5.2 shows also the ratio of convection to overall heat transfer. As mentioned before, HWA is based on convective heat transfer from a heated wire and heat is generated inside that wire owing to its resistance when electrical current passes. So, it is important to calculate amount of heat transferred to the fluid by convection, as compared with the total. This ratio rises with increasing with velocity and aspect ratio. Ratio can be called as φ. For example, φ is equal to 0,913 for the condition of 3.75 mm in length. It means that 9% of heat generated in the sensor by the electric current is conducted to the supports, while almost 91% is transferred to the fluid by convection.

Li (2004) showed the relation between Reynolds number and ratio, φ (see Figure 3.9). φ increases with Reynolds number like present results. This again comes from the relatively smaller conductive heat losses.

Freymuth (1979) introduced the this ratio

$$\epsilon = 1 - \frac{(T_m - T_s)/(T_m - T_a)}{\xi[1+\alpha(T_m - T_a)] + (T_m - T_s)/(T_m - T_a) - 1 + \alpha(T_a - T_s)} \qquad (5.2)$$

Goldstein (1996) used Equation (5.2) and found that ϵ is equal to 0.826 for the condition of 1.25 mm in length and 4 μm in diameter (see Figure 1.10). The system code developed for the present computations is also used to calculate the ratio for this

condition. The ratio, 0.8261 is exactly same as the result of Goldstein (1996). This result shows the importance of Freymuth (1979) theory.

Table 5.3. Conductive heat transfer comparison of single wire and wire with copper-plated ends for various length.

Length [mm]	Velocity [m/s]	Single wire [W]	Single wire with copper-plated ends [W]	Percent reduction [%]
0,3	5	0,02612280	0,02116460	18,98
0,5	5	0,01642030	0,01431810	12,80
1,0	5	0,01187330	0,01073050	9,62
2,0	5	0,00733524	0,00686970	6,35
3,75	5	0,00656373	0,00618090	5,83

Table 5.3 gives the results of conduction to the supports for single wire (unplated ends) and wire with copper-plated ends. Single wire calculations assumes relatively massive support whose temperature, T' is equal to T_a. Therefore, support temperature is not affected by conduction from the wire. When sensitive part of the heated wires is insulated from the supports by a plated area, its temperature no longer is equal to ambient. Supports are assumed to be started at the plating and their temperature, called junction temperature is above the ambient. It is between the plated area and the sensitive part of the wire. Goldstein (1996) says that this can only reduce to conduction losses. Present investigation shows that conduction to the supports is decreased by a plated ends. By this way, temperature distribution along the copper-plated wire (black one) becomes more uniform than unplated wires (see Figure 5.27). This reduction is considerable amount in short wires. Moreover, Dantec Dynamics Inc. notes in “Probes for Hot-wire Anemometry” that the plating of the ends serves dual aim of accurately defining the sensing length and reducing the amount of heat dissipated by the prongs. Another advantage is that flow interference from the prongs is reduced owing to the wider prong spacing.

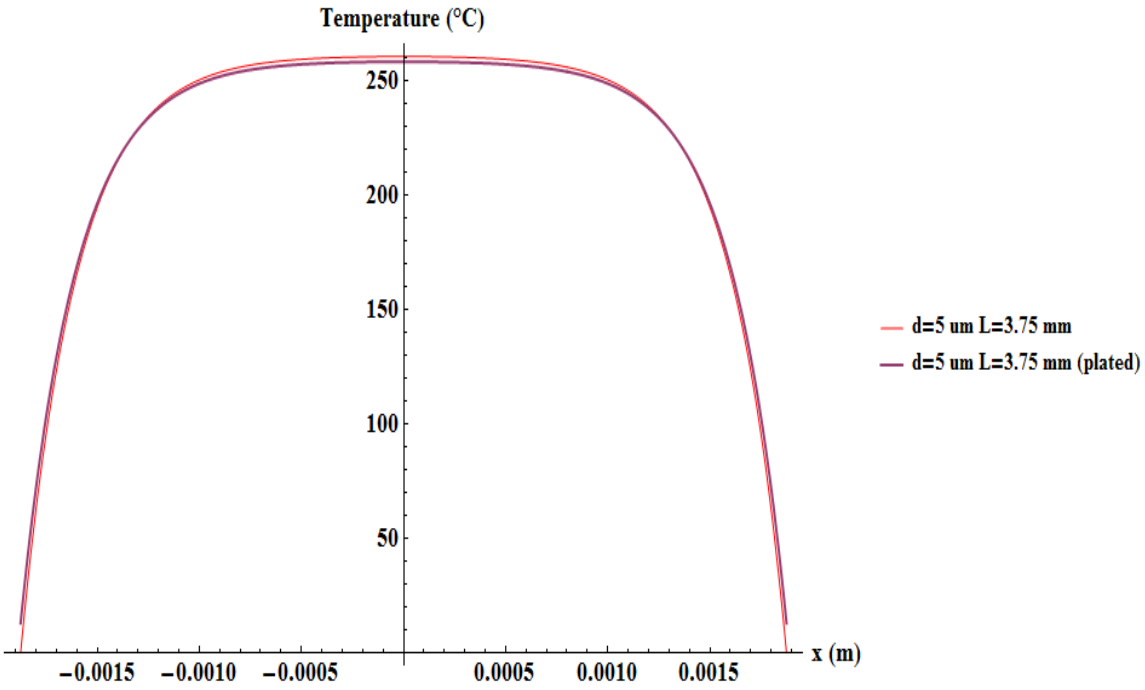

Figure 5.27. Comparison of stationary temperature distribution along the single wire and wire with copper-plated ends.

CHAPTER 6

CONCLUSION

Static behavior and dynamic response of constant temperature hot-wire anemometer has been investigated in this thesis. The analytical and numerical solutions in static analysis for heat transfer from hot-wire indicate that the temperature distribution along a hot-wire depends on length and diameter. Increasing the wire length and decreasing the wire diameter will cause the uniformity of temperature distribution to be increased. Therefore, it provides to reduce thermal transient effects and agrees with the previous works which have been carried out by Davies & Fisher (1964), A. Al-Salaymeh (2005) and Manshadi & Esfeh (2012). Also, present results show that radiation term can be neglected in calculations.

In dynamic part, response of hot-wire is affected by the variation of the heat transfer coefficient. Sensitivity and frequency characteristic of the wire has been studied. Physical meaning of sensitivity is that the reaction of the anemometer power on small harmonic fluctuations of the heat transfer coefficient. Sensitivity of the wire increases with decreasing length and increasing diameter. Reaction would be higher in large diameter because of large heat capacity and therefore, high thermal inertia. However, a uniform frequency response provides more sensitivity over the range of interest for accurate turbulent measurements. So, a key point is the deviation of the flat characteristic of response. According to present results, this behavior favors the use of small diameters (low thermal inertia) and short wires. The agreement the Soe Min Khine *et. al*. (2013) response analysis and present results confirm that the diameter of the wire should be chosen a small value to increase range of frequency response, and spatial resolution and to reduce flow interferense and conduction end losses. The length of the wire should be larger to minimize the end conduction losses and to get more uniform temperature distribution. However, there are other important reasons to favor the shorter wires. The present results show that short wires have high sensitivity value and better frequency response. Also, short wires exhibits more spatial resolution to sense micro scale of turbulence. On the other hand, it has already stated that diameter should be taken as at least 2.5 μm is required for minimum strength. So, diameter can be chosen between 2.5 μm and 5 μm for fluid flow operations.

Effect of aspect ratio on dynamic response has been investigated. Aspect ratio, which is between 200 and 430, gave the best response characteristic. Also, current investigation is fit into the given commercial range. Moreover, it is mentioned about importance of what amount of heat transfer to fluid by convection. That ratio, φ, increase with aspect ratio. Therefore, present results show that aspect ratio should be high enough to avoid the effect of thermal inertia and to minimize end conduction losses. The theoretical results agree with the results of Freymuth (1979), Morris and Foss (2003) and Li (2004). The present mathematical model (straight forward expansion) of hot-wire is inadequate in high aspect ratio cases. It needs to be improved to investigate higher aspect ratios. Nayfeh (2008) says that "*the breakdown in the straight forward expansion is due to its failure to account for the nonlinear dependence of the frequency on the nonlinearity*". Also, straightforward expansion causes the explosions on the dynamic response figures in long time. It should be done by using more advanced techniques, such as the Lindstedt-Pointcare technique, the method of renormalization, and the method of multiple scales.

Sensitivity of hot-wire has been studied by varying fluid velocity. Sensitivity decreases with increasing fluid velocity.

Copper-plated wire ends have been investigated in order to see effect on sensitivity and temperature distribution along the wire. In addition, effect of conduction end losses on dynamic response has been studied for hot-wire. It can be concluded that the ends of the short wire can be covered by copper to achieve high sensitivity value for dissipation measurements. Also, temperature distribution becomes more uniform with the copper-plated ends than unplated one. It provides to reduced conduction end losses and therefore; dynamic response of the wire is influenced less, especially in short wires. Because of this reason, high sensitivity values have been observed in short wires.

REFERENCES

Al-Salaymeh, A. (2005). On the Convective Heat Transfer from Circular Cylinders with Applications to Hot-Wire Anemometry. *Int. Journal of Heat and Technology, Vol. 23*(n. 2).

Arts, Tony, Boerrigter, H, Carbonaro, M, Charbonnier, JM, Degrez, G, Olivari, D, . . . Van den Braembussche, RA. (1994). Measurement Techniques in Fluid Dynamics An Introduction.

Beljaars, A. C. M. (1976). Dynamic behaviour of the constant temperature anemometer due to thermal inertia of the wire. *Applied Scientific Research, 32*(5), 509-518. doi: 10.1007/BF00385921

Bender, C.M., & Orszag, S.A. (1999). *Advanced Mathematical Methods for Scientists and Engineers I: Asymptotic Methods and Perturbation Theory*: Springer.

Bruun, H H. (1996). Hot-Wire Anemometry: Principles and Signal Analysis. *Measurement Science and Technology, 7*(10).

Churchill, R.V. (1958). *Operational Mathematics*: McGraw-Hill.

Collis, D. C., & Williams, M. J. (1959). Two-dimensional convection from heated wires at low Reynolds numbers. *Journal of Fluid Mechanics, 6*(03), 357-384.

Davies, P. O. A. L., & Fisher, M. J. (1964). Heat Transfer From Electrically Heated Cylinders. *Proceedings of the Royal Society of London. Series A, Mathematical and Physical Sciences, 280*(1383), 486-527. doi: 10.2307/2414897

de Haan, R. E. (1971). The dynamic calibration of a hot wire by means of a sound wave. *Applied Scientific Research, 24*(1), 335-353. doi: 10.1007/BF00411723

Freymuth, P. (1979). Engineering estimate of heat conduction loss in constant temperature thermal sensors. *TSI Quart, 4*, 3-6.

Goldstein, Richard J. (1996). *Fluid mechanics measurements*: Taylor & Francis.

Hinze, J.O. (1975). *Turbulence*: McGraw-Hill.

King, L. V. (1914). On the Convection of Heat from Small Cylinders in a Stream of Fluid: Determination of the Convection Constants of Small Platinum Wires, with Applications to Hot-Wire Anemometry, *Proc. R. Soc. London, vol. 90*, pp. 563-570.

Li, J D. (2004). Dynamic response of constant temperature hot-wire system in turbulence velocity measurements. *Measurement Science and Technology, 15*(9), 1835.

Lomas, C.G. (2011). *Fundamentals of Hot Wire Anemometry*: Cambridge University Press.

Lowell, H. H. (1950). Design and applications of hot-wire anemometers for steady-state measurements at transonic and supersonic airspeeds. *NACA Tech. Note 2117*. doi: citeulike-article-id:8769997

Manshadi, Mojtaba Dehghan, & Esfeh, Mohammad Kazemi. (2012). Analytical and Experimental Investigation About Heat Transfer of Hot-Wire Anemometry.

Mojtaba Dehghan Manshadi, Mohamad Kazemi Esfeh. (2012). A New Approach about Heat Transfer of Hot-Wire Anemometer. *Applied Mechanics and Materials, 232*, 747-751. doi: 10.4028/www.scientific.net/AMM.232.747

Morris, S. C., & Foss, J. F. (2003). Transient thermal response of a hot-wire anemometer. *Measurement Science and Technology, 14*(3), 251-259.

Nayfeh, A.H. (2008). *Perturbation Methods*: Wiley.

Sandborn, Virgil A. (1972). *Resistance temperature transducers*: Metrology Press Fort Collins.

Soe Minn Khine, Tomoya Houra, Masato Tagawa. (2013). An Adaptive Response Compensation Technique for the Constant-Current Hot-Wire Anemometer. *Open Journal of Fluid Dynamics, Vol. 3*(No. 2), pp. 95-108. doi: 10.4236/ojfd.2013.32013

Yeh, Y., & Cummins, H. Z. (1964). LOCALIZED FLUID FLOW MEASUREMENTS WITH AN He–Ne LASER SPECTROMETER. *Applied Physics Letters, 4*(10), 176-178. doi: doi:http://dx.doi.org/10.1063/1.1753925